Published for SISSA by Springer

Received: October 16, 2016
Accepted: March 12, 2017
Published: April 4, 2017

Search for electroweak production of charginos in final states with two τ leptons in pp collisions at $\sqrt{s} = 8$ TeV

The CMS collaboration

E-mail: cms-publication-committee-chair@cern.ch

Abstract: Results are presented from a search for the electroweak production of supersymmetric particles in pp collisions in final states with two τ leptons. The data sample corresponds to an integrated luminosity between 18.1 fb^{-1} and 19.6 fb^{-1} depending on the final state of τ lepton decays, at $\sqrt{s} = 8$ TeV, collected by the CMS experiment at the LHC. The observed event yields in the signal regions are consistent with the expected standard model backgrounds. The results are interpreted using simplified models describing the pair production and decays of charginos or τ sleptons. For models describing the pair production of the lightest chargino, exclusion regions are obtained in the plane of chargino mass vs. neutralino mass under the following assumptions: the chargino decays into third-generation sleptons, which are taken to be the lightest sleptons, and the sleptons masses lie midway between those of the chargino and the neutralino. Chargino masses below 420 GeV are excluded at a 95% confidence level in the limit of a massless neutralino, and for neutralino masses up to 100 GeV, chargino masses up to 325 GeV are excluded at 95% confidence level. Constraints are also placed on the cross section for pair production of τ sleptons as a function of mass, assuming a massless neutralino.

Keywords: Hadron-Hadron scattering (experiments), Supersymmetry

ArXiv ePrint: 1610.04870

Open Access, Copyright CERN,
for the benefit of the CMS Collaboration.
Article funded by SCOAP^3.

doi:10.1007/JHEP04(2017)018

Contents

1 Introduction 1

2 The CMS detector and event reconstruction 3

3 The Monte Carlo samples 4

4 Definition of M_{T2} 5

5 Event selection for the $\tau_h\tau_h$ channel 6

6 Event selection for the $\ell\tau_h$ channel 7

7 Backgrounds 7
- 7.1 The QCD multijet background estimation in the $\tau_h\tau_h$ channel 8
- 7.2 W+jets background estimation in the $\tau_h\tau_h$ channel 10
- 7.3 The Drell-Yan background estimation 11
- 7.4 Misidentified τ_h in the $\ell\tau_h$ channels 11

8 Systematic uncertainties 13

9 Results and interpretation 14

10 Summary 16

A Additional information for new model testing 21

The CMS collaboration 30

JHEP04(2017)018

1 Introduction

Supersymmetry (SUSY) [1–5] is one of the most promising extensions of the standard model (SM) of elementary particles. Certain classes of SUSY models can lead to the unification of gauge couplings at high energy, provide a solution to the gauge hierarchy problem without fine tuning by stabilizing the mass of the Higgs boson against large radiative corrections, and provide a stable dark matter candidate in models with conservation of R-parity. A key prediction of SUSY is the existence of new particles with the same gauge quantum numbers as SM particles but differing by a half-unit in spin (sparticles).

Extensive searches at the LHC have excluded the existence of strongly produced (colored) sparticles in a broad range of scenarios, with lower limits on sparticle masses ranging up to 1.8 TeV for gluino pair production [6–13]. While the limits do depend on the details

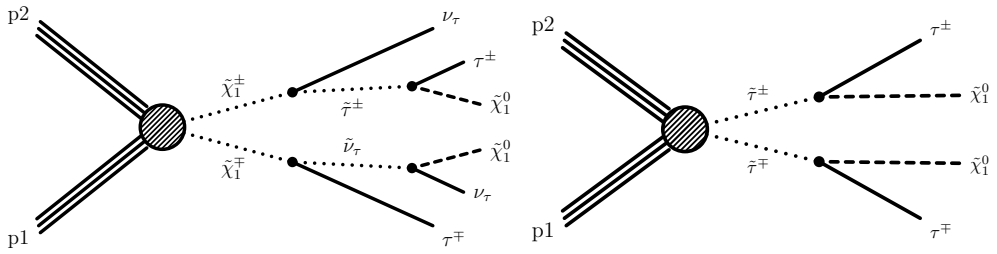

Figure 1. Schematic production of τ lepton pairs from chargino (left) or τ slepton (right) pair production.

of the assumed SUSY particle mass spectrum, constraints on the colorless sparticles are generally much less stringent. This motivates the electroweak SUSY search described in this paper.

Searches for charginos ($\widetilde{\chi}^{\pm}$), neutralinos ($\widetilde{\chi}^0$), and sleptons ($\widetilde{\ell}$) by the ATLAS and CMS Collaborations are described in refs. [14–20]. In various SUSY models, the lightest SUSY partners of the SM leptons are those of the third generation, resulting in enhanced branching fractions for final states with τ leptons [21]. The previous searches for charginos, neutralinos, and sleptons by the CMS Collaboration either did not include the possibility that the scalar τ lepton and its neutral partner ($\widetilde{\tau}$ and $\widetilde{\nu}_\tau$) are the lightest sleptons [16], or that the initial charginos and neutralinos are produced in vector-boson fusion processes [18]. An ATLAS search for SUSY in the di-τ channel is reported in ref. [19], excluding chargino masses up to 345 GeV for a massless neutralino ($\widetilde{\chi}_1^0$). The ATLAS results on direct $\widetilde{\tau}$ production is improved and updated in ref. [20].

In this paper, a search for the electroweak production of the lightest charginos ($\widetilde{\chi}_1^{\pm}$) and scalar τ leptons ($\widetilde{\tau}$) is reported using events with two opposite-sign τ leptons and a modest requirement on the magnitude of the missing transverse momentum vector, assuming the masses of the third-generation sleptons are between those of the chargino and the lightest neutralino. Two τ leptons can be generated in the decay chain of $\widetilde{\chi}_1^{\pm}$ and $\widetilde{\tau}$, as shown in figure 1. The results of the search are interpreted in the context of SUSY simplified model spectra (SMS) [22, 23] for both production mechanisms.

The results are based on a data set of proton-proton (pp) collisions at $\sqrt{s} = 8\,\text{TeV}$ collected with the CMS detector at the LHC during 2012, corresponding to integrated luminosities of 18.1 and 19.6 fb^{-1} in different channels. This search makes use of the stransverse mass variable (M_{T2}) [24, 25], which is the extension of transverse mass (M_{T}) to the case where two massive particles with equal mass are created in pairs and decay to two invisible and two visible particles. In the case of this search, the visible particles are both τ leptons. The distribution of M_{T2} reflects the scale of the produced particles and has a longer tail for heavy sparticles compared to lighter SM particles. Hence, SUSY can manifest itself as an excess of events in the high-side tail of the M_{T2} distribution. Final states are considered where two τ leptons are each reconstructed via hadronic decays ($\tau_{\text{h}}\tau_{\text{h}}$), or where only one τ lepton decays hadronically and the other decays leptonically ($\ell\tau_{\text{h}}$, where ℓ is an electron or muon).

JHEP04(2017)018

The paper is organized as follows. The CMS detector, the event reconstruction, and the data sets are described in sections 2 and 3. The M_{T2} variable is introduced in section 4. The selection criteria for the $\tau_{\mathrm{h}}\tau_{\mathrm{h}}$ and $\ell\tau_{\mathrm{h}}$ channels are described in section 5 and 6, respectively. A detailed study of the SM backgrounds is presented in section 7, while section 8 is devoted to the description of the systematic uncertainties. The results of the search with its statistical interpretation are presented in section 9. Section 10 presents the summaries. The efficiencies for the important selection criteria are summarized in appendix A and can be used to interpret these results within other phenomenological models.

2 The CMS detector and event reconstruction

The central feature of the CMS apparatus is a superconducting solenoid of 6 m internal diameter that provides a magnetic field of 3.8 T. Within the solenoid volume are a silicon pixel and strip tracker, a lead tungstate crystal electromagnetic calorimeter, and a brass and scintillator hadron calorimeter, each composed of a barrel and two endcap sections. Muons are measured in gas-ionization detectors embedded in the steel flux-return yoke outside the solenoid. Extensive forward calorimetry complements the coverage provided by the barrel and endcap detectors. A more detailed description of the CMS detector, together with a definition of the coordinate system used and the relevant kinematic variables, can be found in ref. [26].

To be recorded for further study, events from pp interactions must satisfy criteria imposed by a two-level trigger system. The first level of the CMS trigger system, composed of custom hardware processors, uses information from the calorimeters and muon detectors to select the most interesting events in a fixed time interval of less than 4 μs. The high-level trigger processor farm further decreases the event rate from around 100 kHz to less than 1 kHz before data storage [27].

The particle-flow (PF) algorithm [28, 29] reconstructs and identifies each individual particle with an optimized combination of information from the various elements of the CMS detector. Jets are reconstructed from the PF candidates with the anti-k_t clustering algorithm [30] using a distance parameter of 0.5. We apply corrections dependent on transverse momentum (p_{T}) and pseudorapidity (η) to account for residual effects of nonuniform detector response [31]. A correction to account for multiple pp collisions within the same or nearby bunch crossings (pileup interactions) is estimated on an event-by-event basis using the jet area method described in ref. [32], and is applied to the reconstructed jet p_{T}. The combined secondary vertex algorithm [33] is used to identify ("b tag") jets originating from b quarks. This algorithm is based on the reconstruction of secondary vertices, together with track-based lifetime information. In this analysis a working point is chosen such that, for jets with a p_{T} value greater than 60 GeV the efficiency for tagging a jet containing a b quark is 70% with a light-parton jet misidentification rate of 1.5%, and c quark jet misidentification rate of 20%. Scale factors are applied to the simulated events to reproduce the tagging efficiencies measured in data, separately for jets originating from b or c quarks, and from light-flavor partons. Jets with $p_{\mathrm{T}} > 40$ GeV and $|\eta| < 5.0$ and b-tagged jets with $p_{\mathrm{T}} > 20$ GeV and $|\eta| < 2.4$ are considered in this analysis.

JHEP04(2017)018

The PF candidates are used to reconstruct the missing transverse momentum vector $\vec{p}_{\mathrm{T}}^{\,\mathrm{miss}}$, defined as the negative of the vector sum of the transverse momenta of all PF candidates. For each event, $p_{\mathrm{T}}^{\mathrm{miss}}$ is defined as the magnitude of $\vec{p}_{\mathrm{T}}^{\,\mathrm{miss}}$.

Hadronically decaying τ leptons are reconstructed using the hadron-plus-strips algorithm [34]. The constituents of the reconstructed jets are used to identify individual τ lepton decay modes with one charged hadron and up to two neutral pions, or three charged hadrons. Additional discriminators are used to separate τ_{h} from electrons and muons. Prompt τ leptons are expected to be isolated in the detector. To discriminate them from quantum chromodynamics (QCD) jets, an isolation variable [35] is defined by the scalar sum of the transverse momenta of the charged hadrons and photons falling within a cone around the τ lepton momentum direction after correcting for the effect of pileup. The "loose", "medium", and "tight" working points are defined by requiring the value of the isolation variable not to exceed 2.0, 1.0, and 0.8 GeV, respectively. A similar measure of isolation is computed for charged leptons (e or μ), where the isolation variable is divided by the p_{T} of the lepton. This quantity is used to suppress the contribution from leptons produced in hadron decays in jets.

3 The Monte Carlo samples

The SUSY signal processes and SM samples, which are used to evaluate potential background contributions, are simulated using CTEQ6L1 [36] parton distribution functions. To model the parton shower and fragmentation, all generators are interfaced with PYTHIA 6.426 [37]. The SM processes of Z+jets, W+jets, $\mathrm{t\bar{t}}$, and dibosons are generated using the MadGraph 5.1 [38] generator. Single top quark and Higgs boson events are generated with POWHEG 1.0 [39–42]. In the following, the events from Higgs boson production via gluon fusion, vector-boson fusion, or in association with a W or Z boson or a $\mathrm{t\bar{t}}$ pair are referred to as "hX." Later on, the events containing at least one top quark or one Z boson are referred to as "tX" and "ZX," respectively. The masses of the top quark and Higgs boson are set to be 172.5 GeV [43] and 125 GeV [44], respectively. Since the final state arising from the pair production of W bosons decaying into τ leptons is very similar to our signal, in the following figures its contribution is shown as an independent sample labeled as "WW."

In one of the signal samples, pairs of charginos are produced with PYTHIA 6.426 and decayed exclusively to the final states that contain two τ leptons, two τ neutrinos, and two neutralinos, as shown in figure 1 (left). The daughter sparticle in the two-body decay of the $\widetilde{\chi}_1^{\pm}$ can be either a $\widetilde{\tau}$ or $\widetilde{\nu}_\tau$. In this scenario, no decay modes are considered other than those shown in figure 1 (left), so for $\mathrm{m}(\widetilde{\tau}) = \mathrm{m}(\widetilde{\nu}_\tau)$, the two decay chains (via the $\widetilde{\tau}$ or $\widetilde{\nu}_\tau$) have 50% branching fraction. The masses of the $\widetilde{\tau}$ and $\widetilde{\nu}_\tau$ are set to be equal to the mean value of the $\widetilde{\chi}_1^{\pm}$ and $\widetilde{\chi}_1^0$ masses and consequently are produced on mass shell. If the $\widetilde{\tau}$ ($\widetilde{\nu}_\tau$) mass is close to the $\widetilde{\chi}_1^0$ mass, the τ lepton from the $\widetilde{\tau}$ ($\widetilde{\chi}_1^{\pm}$) decay will have a low (high) momentum, resulting in a lower (higher) overall event selection efficiency, producing a weaker (stronger) limit on the chargino mass. In the case where the $\widetilde{\tau}$ ($\widetilde{\nu}_\tau$) mass is close to the $\widetilde{\chi}_1^{\pm}$ mass, the situations are opposite. Of the scenarios in which the τ slepton and the τ sneutrino have the same mass, the scenario with the highest efficiency overall corresponds to the one in

JHEP04(2017)018

which these masses are half-way between the masses of the $\widetilde{\chi}_1^{\pm}$ and $\widetilde{\chi}_1^0$. In the other signal sample, pairs of staus are also produced with PYTHIA 6.426, that decay always to two τ leptons and two neutralinos, figure 1 (right). To improve the modeling of the τ lepton decays, the TAUOLA 1.1.1a [45] package is used for both signal and background events.

In the data set considered in this paper, there are on average 21 pp interactions in each bunch crossing. Such additional interactions are generated with PYTHIA and superimposed on simulated events in a manner consistent with the instantaneous luminosity profile of the data set. The detector response in the Monte Carlo (MC) background event samples is modeled by a detailed simulation of the CMS detector based on GEANT4 [46]. For the simulation of signal events, many samples of events, corresponding to a grid of $\widetilde{\chi}_1^{\pm}$ and $\widetilde{\chi}_1^0$ mass values, must be generated. To reduce computational requirements, signal events are processed by the CMS fast simulation [47] instead of GEANT4. It is verified that the CMS fast simulation is in reasonable agreement with the detailed simulation for our signal which has hadronic decays of tau leptons in the final state. The simulated events are reconstructed with similar algorithms used for collision data.

The yields for the simulated SM background samples are normalized to the cross sections available in the literature. These cross sections correspond to next-to-next-to-leading-order (NNLO) accuracy for Z+jets [48] and W+jets [49] events. For the $\mathrm{t\bar{t}}$ simulated samples, the cross section used is calculated to full NNLO accuracy including the resummation of next-to-next-to-leading-logarithmic (NNLL) terms [50]. The event yields from diboson production are normalized to the next-to-leading-order (NLO) cross section taken from ref. [51]. The RESUMMINO [52–54] program is used to calculate the signal cross sections at NLO+NLL level where NLL refers to next-to-leading-logarithmic precision.

4 Definition of M_{T2}

The M_{T2} variable [24, 25] is used in this analysis to discriminate between the SUSY signal and the SM backgrounds as proposed in ref. [55]. This variable has been used extensively by both CMS and ATLAS in searches for supersymmetry [10, 19]. The variable was introduced to measure the mass of primary pair-produced particles that eventually decay to undetected particles (e.g. neutralinos). Assuming the two primary SUSY particles undergo the same decay chain with visible and undetectable particles in the final state, the system can be described by the visible mass ($m^{\mathrm{vis}(i)}$), transverse energy ($E_{\mathrm{T}}^{\mathrm{vis}(i)}$), and transverse momentum ($\vec{p}_{\mathrm{T}}^{\,\mathrm{vis}(i)}$) of each decay branch ($i = 1, 2$), together with the $\vec{p}_{\mathrm{T}}^{\,\mathrm{miss}}$, which is shared between the two decay chains. The quantity $\vec{p}_{\mathrm{T}}^{\,\mathrm{miss}}$ is interpreted as the sum of the transverse momenta of the neutralinos, $\vec{p}_{\mathrm{T}}^{\,\widetilde{\chi}_1^0(i)}$. In decay chains with neutrinos, $\vec{p}_{\mathrm{T}}^{\,\mathrm{miss}}$ also includes contributions from the $\vec{p}_{\mathrm{T}}$ of the neutrinos.

The transverse mass of each branch can be defined as

$$\left(M_{\mathrm{T}}{}^{(i)}\right)^2 = \left(m^{\mathrm{vis}(i)}\right)^2 + m_{\widetilde{\chi}_1^0}^2 + 2\left(E_{\mathrm{T}}^{\mathrm{vis}(i)} E_{\mathrm{T}}^{\widetilde{\chi}_1^0(i)} - \vec{p}_{\mathrm{T}}^{\,\mathrm{vis}(i)} . \vec{p}_{\mathrm{T}}^{\,\widetilde{\chi}_1^0(i)}\right). \tag{4.1}$$

For a given $m_{\widetilde{\chi}_1^0}$, the M_{T2} variable is defined as

$$M_{\mathrm{T2}}(m_{\widetilde{\chi}_1^0}) = \min_{\vec{p}_{\mathrm{T}}^{\,\widetilde{\chi}_1^0(1)} + \vec{p}_{\mathrm{T}}^{\,\widetilde{\chi}_1^0(2)} = \vec{p}_{\mathrm{T}}^{\,\mathrm{miss}}} \left[\max\left\{M_{\mathrm{T}}{}^{(1)}, M_{\mathrm{T}}{}^{(2)}\right\}\right]. \tag{4.2}$$

JHEP04(2017)018

For the correct value of $m_{\widetilde{\chi}_1^0}$, the kinematic endpoint of the M_{T2} distribution is at the mass of the primary particle [56, 57], and it shifts accordingly when the assumed $m_{\widetilde{\chi}_1^0}$ is lower or higher than the correct value. In this analysis, the visible part of the decay chain consists of either the two τ_h ($\tau_\mathrm{h}\tau_\mathrm{h}$ channel) or a combination of a muon or an electron with a τ_h candidate ($\ell\tau_\mathrm{h}$ channel), so $m^{\mathrm{vis}(i)}$ is the mass of a lepton and can be set to zero. We also set $m_{\widetilde{\chi}_1^0}$ to zero.

The background processes with a back-to-back topology of $\tau_\mathrm{h}\tau_\mathrm{h}$ or $\ell\tau_\mathrm{h}$ are expected from Drell-Yan (DY) or dijet events where two jets are misidentified as $\tau_\mathrm{h}\tau_\mathrm{h}$ or $\ell\tau_\mathrm{h}$. The resulting M_{T2} value is close to zero with our choices of $m_{\widetilde{\chi}_1^0}$ and $m^{\mathrm{vis}(i)}$, regardless of the values of $p_\mathrm{T}^{\mathrm{miss}}$ and the p_T of the τ candidates. This is not the case for signal events, where the leptons are not in a back-to-back topology because of the presence of two undetected neutralinos.

5 Event selection for the $\tau_\mathrm{h}\tau_\mathrm{h}$ channel

In this channel data of pp collisions, corresponding to an integrated luminosity of 18.1 fb^{-1}, are used. The events are first selected with a trigger [58] that requires the presence of two isolated τ_h candidates with $p_\mathrm{T} > 35\,\mathrm{GeV}$ and $|\eta| < 2.1$, passing loose identification requirements. Offline, the two τ_h candidates must pass the medium τ isolation discriminator, $p_\mathrm{T} > 45\,\mathrm{GeV}$ and $|\eta| < 2.1$, and have opposite sign (OS). In events with more than one $\tau_\mathrm{h}\tau_\mathrm{h}$ pair, only the pair with the most isolated τ_h objects is considered.

Events with extra isolated electrons or muons of $p_\mathrm{T} > 10\,\mathrm{GeV}$ and $|\eta| < 2.4$ are rejected to suppress backgrounds from diboson decays. Inspired from the MC studies, the contribution from the $\mathrm{Z} \to \tau_\mathrm{h}\tau_\mathrm{h}$ background is reduced by rejecting events where the visible di-τ_h invariant mass is between 55 and 85 GeV (Z boson veto). Furthermore, contributions from low-mass DY and QCD multijet production are reduced by requiring the invariant mass to be greater than 15 GeV . To further reduce $\mathrm{Z} \to \tau_\mathrm{h}\tau_\mathrm{h}$ and QCD multijet events, $p_\mathrm{T}^{\mathrm{miss}} > 30\,\mathrm{GeV}$ and $M_{\mathrm{T2}} > 40\,\mathrm{GeV}$ are also required. The minimum angle $\Delta\phi$ in the transverse plane between the $\vec{p}_\mathrm{T}^{\mathrm{miss}}$ and any of the τ_h and jets, including b-tagged jets, must be greater than 1.0 radians. This requirement reduces backgrounds from QCD multijet events and W+jets events.

After applying the preselection described above, additional requirements are introduced to define two search regions. The first search region (SR1) targets models with a large mass difference (Δm) between charginos and neutralinos. In this case, the M_{T2} signal distribution can have a long tail beyond the distribution of SM backgrounds. The second search region (SR2) is dedicated to models with small values of Δm. In this case, the sum of the two transverse mass values, $\Sigma M_\mathrm{T}^{\tau_i} = M_\mathrm{T}(\tau_\mathrm{h}^1, \vec{p}_\mathrm{T}^{\mathrm{miss}}) + M_\mathrm{T}(\tau_\mathrm{h}^2, \vec{p}_\mathrm{T}^{\mathrm{miss}})$, provides additional discrimination between signal and SM background processes.

The two signal regions (SR) are defined as:

- SR1: $M_{\mathrm{T2}} > 90\,\mathrm{GeV}$;
- SR2: $M_{\mathrm{T2}} < 90\,\mathrm{GeV}$, $\Sigma M_\mathrm{T}^{\tau_i} > 250\,\mathrm{GeV}$, and events with b-tagged jets are vetoed.

JHEP04(2017)018

The veto on events containing b-tagged jets in SR2 reduces the number of $t\bar{t}$ events, which are expected in the low-M_{T2} region. Table 1 summarizes the selection requirements for the different signal regions.

6 Event selection for the $\ell\tau_h$ channel

Events in the $\ell\tau_h$ final states ($e\tau_h$ and $\mu\tau_h$) are collected with triggers that require a loosely isolated τ_h with $p_T > 20\,\text{GeV}$ and $|\eta| < 2.3$, as well as an isolated electron or muon with $|\eta| < 2.1$ [58–60]. The minimum p_T requirement for the electron (muon) was increased during the data taking from 20 to 22 GeV (17 to 18 GeV) due to the increase in instantaneous luminosity. An integrated luminosity of $19.6\,\text{fb}^{-1}$ is used to study these channels.

In the offline analysis, the electron, muon, and τ_h objects are required to have $p_T > 25$, 20, and 25 GeV, respectively, and the corresponding identification and isolation requirements are tightened. The $|\eta|$ requirements are the same as those in the online selections. In events with more than one opposite-sign $\ell\tau_h$ pair, only the pair that maximizes the scalar p_T sum of τ_h and electron or muon is considered. Events with additional loosely isolated leptons with $p_T > 10\,\text{GeV}$ are rejected to suppress backgrounds from Z boson decays.

Just as for the $\tau_h\tau_h$ channel, preselection requirements to suppress QCD multijet, $t\bar{t}$, $Z \to \tau\tau$, and low-mass resonance events are applied. These requirements are $\ell\tau_h$ invariant mass between 15 and 45 GeV or $> 75\,\text{GeV}$ (Z boson veto), $p_T^{\text{miss}} > 30\,\text{GeV}$, $M_{T2} > 40\,\text{GeV}$, and $\Delta\phi > 1.0$ radians. The events with b-tagged jets are also rejected to reduce the $t\bar{t}$ background. The final signal region requirements are $M_{T2} > 90\,\text{GeV}$ and $M_T^{\tau_h} > 200\,\text{GeV}$. The latter requirement provides discrimination against the W+jets background. Unlike in the $\tau_h\tau_h$ channel, events with $M_{T2} < 90\,\text{GeV}$ are not used because of the higher level of background.

The summary of the selection requirements is shown in table 1. Figure 2 shows the M_{T2} distribution after the preselection requirements are imposed. The data are in good agreement with the SM expectations, evaluated from MC simulation, within the statistical uncertainties. A SUSY signal corresponding to high Δm ($m_{\widetilde{\chi}_1^\pm} = 380\,\text{GeV}$, $m_{\widetilde{\chi}_1^0} = 1\,\text{GeV}$) is used to show the expected signal distribution.

7 Backgrounds

The backgrounds are studied in two categories: those with "misidentified" τ_h, i.e., events where a quark or gluon jet has been misidentified as a τ_h, and those with genuine τ_h candidates. The QCD multijet and W+jets events are the dominant sources in the first category, while a mixture of $t\bar{t}$, Z+jets, diboson, and Higgs boson events dominate the second category. Background estimates are performed using control samples in data whenever possible. Those backgrounds that are taken from simulation are either validated in dedicated control regions or corrected using data-to-simulation scale factors. The estimates of the main backgrounds are discussed below, while the remaining contributions are small and are taken from simulation.

JHEP04(2017)018

$\ell\tau_h$	$\tau_h\tau_h$ SR1	$\tau_h\tau_h$ SR2
OS $\ell\tau_h$	OS $\tau_h\tau_h$	
Extra lepton veto Invariant mass of $\ell\tau_h$ or $\tau_h\tau_h > 15\,\text{GeV}$ Z boson mass veto $p_T^{\text{miss}} > 30\,\text{GeV}$ $M_{T2} > 40\,\text{GeV}$ $\Delta\phi > 1.0\,\text{radians}$		
b-tagged jet veto $M_{T2} > 90\,\text{GeV}$ $M_T^{\tau_h} > 200\,\text{GeV}$	— —	b-tagged jet veto $M_{T2} < 90\,\text{GeV}$ $\Sigma M_T^{\tau_i} > 250\,\text{GeV}$

Table 1. Definition of the signal regions.

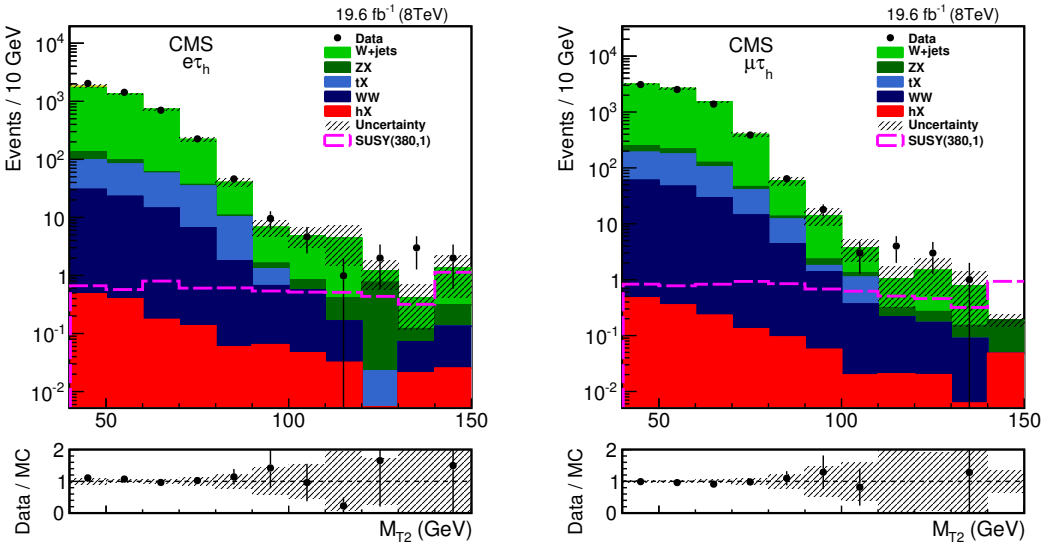

Figure 2. The M_{T2} distribution before applying the final selections on M_{T2} and $M_T^{\tau_h}$, compared to SM expectation in (left) eτ_h and (right) $\mu\tau_h$ channels. The signal distribution is shown for $m_{\tilde{\chi}_1^\pm} = 380\,\text{GeV}, m_{\tilde{\chi}_1^0} = 1\,\text{GeV}$. The last bins include all overflows to higher values of M_{T2}. Only the statistical uncertainties are shown.

7.1 The QCD multijet background estimation in the $\tau_h\tau_h$ channel

Events from QCD multijet production can appear in the signal regions if two hadronic jets are misidentified as a $\tau_h\tau_h$ pair. The isolation variable is a powerful discriminant between misidentified and genuine τ_h candidates. To estimate the QCD multijet contribution, an ABCD method is used, where three $\tau_h\tau_h$ control regions (CRs) are defined using the loose τ_h isolation requirement, together with lower thresholds on M_{T2} or $\Sigma M_T^{\tau_i}$ variables for the corresponding signal region. The former is changed from $M_{T2} > 90$ to $>40\,\text{GeV}$, whereas the latter is reduced from $\Sigma M_T^{\tau_i} > 250$ to $>100\,\text{GeV}$. In addition, the requirement on

JHEP04(2017)018

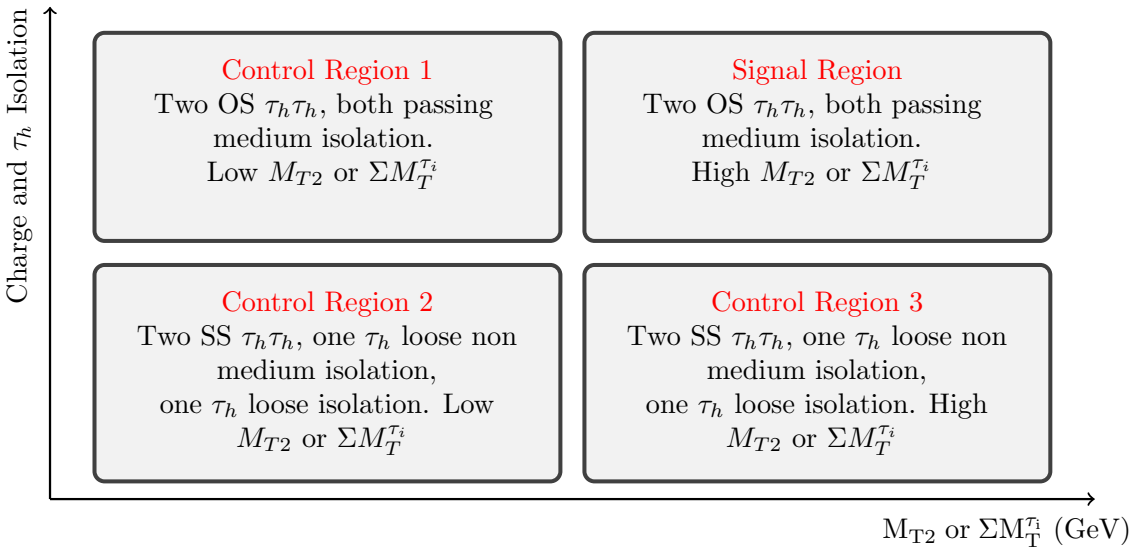

Figure 3. Schematic illustration of three control regions and the signal region used to estimate the QCD multijet background.

$\Delta\phi$ is removed to increase the number of events in the CRs. To reduce contamination from genuine $\tau_h\tau_h$ events in CRs with at least one loose τ_h candidate, same-sign (SS) $\tau_h\tau_h$ pairs are selected. Residual contributions from genuine $\tau_h\tau_h$ and W+jets events (non-QCD events) are subtracted based on MC expectations. The CR and signal region are illustrated in figure 3. In the samples dominated by QCD multijet events (CR1 and CR2), the isolation of misidentified τ_h candidates is found to be uncorrelated with the search variables M_{T2} and $\Sigma M_T^{\tau_i}$. The QCD multijet background in the signal regions is therefore estimated by scaling the number of QCD multijet events with high M_{T2} or high $\Sigma M_T^{\tau_i}$ and loosely isolated SS $\tau_h\tau_h$ (CR3) by a transfer factor, which is the y-intercept of a horizontal line fitted to the ratio of the numbers of events in CR1 and CR2 in different bins of the low values of the search variables. The final estimate of the background is corrected for the efficiency of the $\Delta\phi$ requirement for QCD multijet events. This efficiency is measured in CR1 and CR2, in which the contribution of QCD multijet events is more than 80%. It is checked that the efficiency versus the search variable is same in both CR1 and CR2 and to gain in statistics, two CRs are combined before measuring the efficiency. The efficiency is a falling distribution as a function of the search variable (M_{T2} or $\Sigma M_T^{\tau_i}$) and the value of the last bin ($65 < M_{T2} < 90$ GeV or $200 < \Sigma M_T^{\tau_i} < 250$ GeV) is used conservatively as the value of the efficiency in the signal regions.

The number of data events in CR3 after subtracting the non-QCD events is 4.81 $\pm$ 2.57 (8.62 $\pm$ 3.55) for the SR1 (SR2) selection. For SR1 (SR2), the transfer factors and $\Delta\phi$ efficiencies are measured to be 0.91 $\pm$ 0.12 (0.89 $\pm$ 0.11) and 0.03 $^{+0.04}_{-0.03}$ (0.15 $\pm$ 0.08), respectively. The reported uncertainties are the quadratic sum of the statistical and systematic uncertainties.

The systematic uncertainty in the background estimates includes the uncertainty in the validity of the assumption that isolation and M_{T2} or $\Sigma M_T^{\tau_i}$ are not correlated, the

JHEP04(2017)018

Signal region	QCD multijet background estimate
$\tau_h\tau_h$ SR1	$0.13 \pm 0.06\,(\text{stat})^{+0.18}_{-0.13}\,(\text{syst}) \pm 0.10\,(\text{fit})$
$\tau_h\tau_h$ SR2	$1.15 \pm 0.39\,(\text{stat}) \pm 0.70\,(\text{syst}) \pm 0.25\,(\text{fit})$

Table 2. The estimated QCD multijet background event yields in the $\tau_h\tau_h$ channel. The first two uncertainties are the statistical and systematic uncertainties of the method, and the last uncertainty is the extra systematic uncertainty due to the correlation assumptions.

$\Delta\phi$ efficiency is extrapolated correctly to the signal regions, and the uncertainties in the residual non-QCD SM backgrounds which are subtracted based on MC expectations for different components of the background estimation. The latter includes both the statistical uncertainty of the simulated events and also a 22% systematic uncertainty that will be discussed in section 8, assigned uniformly to all simulated events.

Table 2 summarizes the estimation of the QCD multijet background contribution in the two signal regions after extrapolation from the control regions and correcting for the $\Delta\phi$ efficiency. To evaluate the uncertainties in the transfer factor and $\Delta\phi$ efficiency due to the correlation assumptions, different fit models are examined: (i) a horizontal line or a line with a constant slope is fitted in the distributions of the transfer factor or $\Delta\phi$ efficiency for $40 < M_{T2} < 90\,\text{GeV}$ in the SR1 case ($100 < \Sigma M_T^{\tau_i} < 250\,\text{GeV}$ in the SR2 case); or (ii) the value of the last bin adjacent to the signal region is used. The weighted average of the estimates is compared with the reported values in table 2 to extract the "fit" uncertainty.

7.2 W+jets background estimation in the $\tau_h\tau_h$ channel

In the $\tau_h\tau_h$ channel, the number of remaining events for W+jets from MC is zero, but it has a large statistical uncertainty due to the lack of the statistics in the simulated sample. To have a better estimation, the contribution of the W+jets background in the $\tau_h\tau_h$ channel is taken from simulated events, using the formula:

$$N_{SR} = \epsilon_{FS} N_{BFS}. \tag{7.1}$$

Here N_{SR} is the estimation of W+jets events in the signal region, N_{BFS} is the number of W+jets events before applying the final selection criterion ($M_{T2} > 90\,\text{GeV}$ for SR1 and $\Sigma M_T^{\tau_i} > 250\,\text{GeV}$ for SR2), but after applying all other selection criteria, including $M_{T2} > 40\,\text{GeV}$ for SR1 and $40 < M_{T2} < 90\,\text{GeV}$ for SR2. The efficiency of the final selection (ϵ_{FS}) is defined as $N(M_{T2} > 90)/N(M_{T2} > 40)$ for SR1 and $N(\Sigma M_T^{\tau_i} > 250)/N(40 < M_{T2} < 90)$ for SR2. The value of N_{BFS} is 31.9 ± 6.4 (29.1 ± 6.2) for SR1 (SR2), where the uncertainties arise from the limited number of simulated events.

The ϵ_{FS} is evaluated in a simulated W+jets sample with a pair of opposite-sign τ_h candidates, where the τ_h candidates are selected with the same identification requirements as in the signal region, but with looser kinematic selection criteria to improve statistical precision. Additional signal selection requirements on $\Delta\phi$ or the lepton veto are applied one by one such that two orthogonal subsamples (passing and failing) are obtained. The ϵ_{FS} quantity is calculated in all subsamples. The values are consistent with those obtained from the sample defined with relaxed requirements within the statistical uncertainties. The

JHEP04(2017)018

Signal Region	W+jets background estimate
$\tau_h\tau_h$ SR1	$0.70 \pm 0.21\,(\text{stat}) \pm 0.09\,(\text{syst}) \pm 0.54\,(\text{shape})$
$\tau_h\tau_h$ SR2	$4.36 \pm 1.05\,(\text{stat}) \pm 1.14\,(\text{syst}) \pm 1.16\,(\text{shape})$

Table 3. The W+jets background estimate in the two search regions. The systematic uncertainty "syst" comes from the maximum variation of the estimation found from varying the τ_h energy scale within its uncertainty. The "shape" uncertainty takes into account the difference between the shape of the search variable distribution in data and simulation.

measured ϵ_{FS} values from the looser-selection samples are 0.028 ± 0.010 and 0.098 ± 0.032 for SR1 and SR2, respectively. The uncertainty in the τ_h energy scale is also taken into account in the uncertainty in ϵ_{FS}.

The W+jets simulated sample is validated in data using a same-sign $\mu\tau_h$ control sample, where both the normalization and ϵ_{FS} are checked. The ratio of data to MC expectation is found to be $1.05 \pm 0.13\,(1.02 \pm 0.09)$ for SR1 (SR2), which is compatible with unity within the uncertainties. For ϵ_{FS}, to take into account the difference between the data and MC values, the MC prediction in each of the two signal regions is corrected by the ratio of $\epsilon_{FS(data)}$ to $\epsilon_{FS(MC)}$, which is $0.73 \pm 0.57\,(1.49 \pm 0.38)$ for SR1 (SR2), and its uncertainty is also taken to be the "shape" systematic uncertainty.

Table 3 summarizes the estimated results for different signal regions for the $\tau_h\tau_h$ channel.

7.3 The Drell-Yan background estimation

The DY background yield is obtained from the MC simulation. The simulated sample includes production of different lepton pairs (ee, $\mu\mu$, and $\tau\tau$). The contribution from $Z \to \ell\ell$ and $Z \to \tau\tau \to \ell\ell$ events is found to be very small, because the misidentification probabilities for $\ell \to \tau_h$ are sufficiently low. The dominant background events are $Z \to \tau\tau \to \ell\tau_h$ and $Z \to \tau\tau \to \tau_h\tau_h$ decays. The misidentification probability for $\tau_h \to \ell$ is also low, so the probability to have DY background contribution from $Z \to \tau\tau \to \tau_h\tau_h$ events in the $\ell\tau_h$ channels is negligible. The simulation is validated in a $\mu\tau_h$ control region obtained by removing the $\Delta\phi$ requirement and by inverting the Z boson veto and also by requiring $M_{T2} < 20\,\text{GeV}$, $40 < M_T^{\tau_h} < 100\,\text{GeV}$. The distributions of the invariant mass of the $\mu\tau_h$ system for data and simulated events are in good agreement. The p_T of the Z boson system, which is correlated with M_{T2}, is also well reproduced in simulation. Table 4 summarizes the DY background contribution in the different signal regions. For $\ell\tau_h$ channels, only the contributions from the genuine lepton+τ_h are reported. A separate method is developed in section 7.4 to estimate the misidentified lepton contamination in these channels. The systematic uncertainties of the DY background are discussed in detail in section 8.

7.4 Misidentified τ_h in the $\ell\tau_h$ channels

The contribution from misidentified τ_h in the $\ell\tau_h$ channels is estimated using a method which takes into account the probability that a loosely isolated misidentified or genuine τ_h passes the tight isolation requirements. If the signal selection is done using the τ_h

JHEP04(2017)018

Signal Region	DY background estimate
$e\tau_h$	0.19 ± 0.04
$\mu\tau_h$	0.25 ± 0.06
$\tau_h\tau_h$ SR1	0.56 ± 0.07
$\tau_h\tau_h$ SR2	0.81 ± 0.56

Table 4. The DY background contribution estimated from simulation in four signal regions. The uncertainties are due to the limited number of MC events.

candidates that pass the loose isolation, the number of loose τ_h candidates (N_l) is:

$$N_l = N_g + N_m \tag{7.2}$$

where N_g is the number of genuine τ_h candidates and N_m is the number of misidentified τ_h candidates. If the selection is tightened, the number of tight τ_h candidates (N_t) is

$$N_t = r_g N_g + r_m N_m \tag{7.3}$$

where r_g (r_m) is the genuine (misidentified τ_h) rate, i.e., the probability that a loosely selected genuine (misidentified) τ_h candidate passes the tight selection. One can obtain the following expression by eliminating N_g:

$$r_m N_m = r_m(N_t - r_g N_l)/(r_m - r_g). \tag{7.4}$$

Here, the product $r_m N_m$ is the contamination of misidentified τ_h candidates in the signal region. This is determined by measuring r_m and r_g along with the number of loose τ_h candidates (N_l) and the number of tight τ_h candidates (N_t).

The misidentification rate (r_m) is measured as the ratio of tightly selected τ_h candidates to loosely selected τ_h candidates in a sample dominated by misidentified τ_h candidates. This is done in a data sample with the same selection as $\ell\tau_h$, except with an inverted p_T^{miss} requirement, i.e., $p_T^{miss} < 30\,GeV$. The misidentification rate is measured to be 0.54 ± 0.01. The genuine τ_h candidate rate (r_g) is estimated in simulated DY events; it is found to be $r_g = 0.766 \pm 0.003$ and almost independent of M_{T2}. A relative systematic uncertainty of 5% is assigned to the central value of r_g to cover its variations for different values of M_{T2}. The method is validated in the simulated W+jets sample using the misidentification rate which is evaluated with the same method as used for data. This misidentification rate is $r_m = 0.51$. This difference is taken as the systematic uncertainty of 5% in the central value of the misidentification rate ($r_m = 0.54$). The method predicts the number of $\ell\tau_h$ background events in this sample within the uncertainties. These include statistical uncertainties due to the number of events in the sidebands (loosely selected τ_h candidates), as well as systematic uncertainties. The uncertainties in the misidentification rate and the genuine τ_h candidate rate are negligible compared to the statistical uncertainties associated to the control regions.

The estimates of the misidentified τ_h contamination in the two $\ell\tau_h$ channels are summarized in table 5. The relative statistical and systematic uncertainties are reported separately. Since the same misidentified and genuine τ_h candidate rates are used to estimate

JHEP04(2017)018

Channel	Total misid (events)	Stat (%)	r_m syst (%)	r_g syst (%)	Total uncert (%)
$e\tau_h$	3.30	101	17	2	102
$\mu\tau_h$	8.15	56	18	5	59

Table 5. Estimation of the misidentified τ_h contribution in the signal region of the $\ell\tau_h$ channels. The total systematic uncertainty is the quadratic sum of the individual components. All uncertainties are relative. The r_m (r_g) is shorthand for misidentified (genuine) τ_h candidate rate.

the backgrounds for both the $e\tau_h$ and $\mu\tau_h$ channels, the total systematic uncertainties are considered fully correlated between the two channels. The numbers of misidentified events (3.30 for the $e\tau_h$ channel and 8.15 for the $\mu\tau_h$ channel) are consistent within the statistical uncertainties in our control samples.

8 Systematic uncertainties

Systematic uncertainties can affect the shape or normalization of the backgrounds estimated from simulation ($t\bar{t}$, Z+jets, diboson, and Higgs boson events), as well as the signal acceptance. Systematic uncertainties of other background contributions are described in sections 7.1, 7.2 and 7.4. The uncertainties are listed below, and summarized in table 6.

- The energy scales for electron, muon, and τ_h objects affect the shape of the kinematic distributions. The systematic uncertainties in the muon and electron energy scales are negligible. The visible energy of τ_h object in the MC simulation is scaled up and down by 3%, and all τ_h-related variables are recalculated. The resulting variations in final yields are taken as the systematic uncertainties. They are evaluated to be 10–15% for backgrounds and 2–15% in different parts of the signal phase space.

- The uncertainty in the τ_h identification efficiency is 6%. The uncertainty in the trigger efficiency of the τ_h part of the $e\tau_h$ and $\mu\tau_h$ ($\tau_h\tau_h$) triggers amounts to 3.0% (4.5%) per τ_h candidate. A "tag-and-probe" technique [61] on $Z \to \tau\tau$ data events is used to estimate these uncertainties [35].

- The uncertainty in electron and muon trigger, identification, and isolation efficiencies is 2% [35].

- The uncertainty due to the scale factor for the b-tagging efficiency and misidentification rate is evaluated by varying the factors within their uncertainties. The yields of signal and background events are changed by 8% and 4%, respectively [33].

- To evaluate the uncertainty due to pileup, the measured inelastic pp cross section is varied by 5% [62], resulting in a change in the number of simulated pileup interactions. The relevant efficiencies for signal and background events are changed by 4%.

- The uncertainty in the signal acceptance due to parton distribution function (PDF) uncertainties is taken to be 2% from a similar analysis [16] which follows the PDF4LHC recommendations [63].

JHEP04(2017)018

- The uncertainty in the integrated luminosity is 2.6% [64]. This affects only the normalization of the signal MC samples. Because for the backgrounds either control samples in data are used or the normalization is measured from data.

- The uncertainty in the signal acceptance associated with initial-state radiation (ISR) is evaluated by comparing the efficiencies of jet-related requirements in the MadGraph+pythia program. Using the SM WW process, which is expected to be similar to chargino pair production in terms of parton content and process, a 3% uncertainty in the efficiency of b-tagged jets veto and a 6% uncertainty in the $\Delta\phi$ requirement are assigned.

- The uncertainties related to $p_{\mathrm{T}}^{\mathrm{miss}}$ can arise from different sources, e.g. the energy scales of lepton, τ_{h}, and jet objects, and unclustered energy. The unclustered energy is the energy of the reconstructed objects which do not belong to any jet or lepton with $p_{\mathrm{T}} > 10\,\mathrm{GeV}$. The effect of lepton and τ_{h} energy scales is discussed above. The contribution from the uncertainty in the jet energy scale (2–10% depending on η and p_{T}) and unclustered energy (10%) is found to be negligible. A conservative value of 5% uncertainty is assigned to both signal and background processes based on MC simulation studies [16, 18].

- The performance of the fast detector simulation has some differences compared to the full detector simulation, especially in track reconstruction [18] that can affect the τ_{h} isolation. A 5% systematic uncertainty per τ_{h} candidate is assigned by comparing the τ_{h} isolation and identification efficiency in the fast and full simulations.

- The statistical uncertainties due to limited numbers of simulated events also contributes to the overall uncertainties. This uncertainty amounts to 3–15% for the different parts of the signal phase space and 13–70% for the backgrounds in different signal regions.

- For less important backgrounds like $\mathrm{t\bar{t}}$, dibosons, and Higgs boson production, the number of simulated events remaining after event selection is very small. A 50% uncertainty is considered for these backgrounds to account for the possible theoretical uncertainty in the cross section calculation as well as the shape mismodeling.

The systematic uncertainties that can alter the shapes are added in quadrature and treated as correlated when two signal regions of the $\tau_{\mathrm{h}}\tau_{\mathrm{h}}$ channel are combined. Other systematic uncertainties of these two channels and all of the systematic uncertainties of the $\ell\tau_{\mathrm{h}}$ channels are treated as uncorrelated.

9 Results and interpretation

The observed data and predicted background yields for the four signal regions are summarized in table 7. There is no evidence for an excess of events with respect to the predicted SM values in any of the signal regions. In SR2, two events are observed while 7.07 events

JHEP04(2017)018

Systematic uncertainty source	Background (%)			Signal (%)		
	$\ell\tau_h$	$\tau_h\tau_h$ SR1	$\tau_h\tau_h$ SR2	$\ell\tau_h$	$\tau_h\tau_h$ SR1	$\tau_h\tau_h$ SR2
τ_h energy scale (*)	10	15		2–12	3–15	
τ_h identification efficiency	6	12		6	12	
τ_h trigger efficiency	3	9		3	9	
Lepton trigger and ident. eff.	2	—		2	—	
b-tagged jets veto	4	—	4	8	—	8
Pileup		4			4	
PDF (*)		—			2	
Integrated luminosity		—			2.6	
ISR (*)		—			3	
$\Delta\phi_{\text{min}}$		—			6	
p_T^{miss} (*)		5			5	
Fast/full τ_h ident. eff.		—		5	10	
Total shape-affecting sys.	11	16	16	6–13	7–16	
Total non-shape-affecting sys.	9	16	16	14	20	21
Total systematic	14	22	22	15–19	21–25	22–26
MC statistics	22	13	70		3–15	
Total	26	26	73	15–24	21–29	22–30
Low-rate backgrounds		50			—	

Table 6. Summary of the systematic uncertainties that affect the signal event selection efficiency, DY and rare backgrounds normalization and their shapes. The sources that affect the shape are indicated by (*) next to their names. These sources are considered correlated between two signal regions of the $\tau_h\tau_h$ analysis in the final statistical combination.

are expected. The dominant background source is W+jets events. As a cross-check, data and the prediction in the sideband ($200 < \Sigma M_T^{\tau_i} < 250\,\text{GeV}$) are studied: 13 events are observed with an expectation of $17.1 \pm 5.0\,(\text{stat+syst})$ events. This result indicates that the difference between the observed and predicted event yields in SR2 can be attributed to a downward fluctuation in the data.

Figure 4 compares the data and the SM expectation in four search regions. The top row shows the M_{T2} distributions in the $\ell\tau_h$ channels. In these plots, the QCD multijet, W+jets, and misidentified lepton contribution from other channels are based on the estimate described in section 7.4 and labeled as W+jets. The bottom row shows the M_{T2} and $\Sigma M_T^{\tau_i}$ distributions in the two different signal regions of the $\tau_h\tau_h$ channel. The QCD multijet contribution in these plots is obtained using control samples in data, as described in section 7.1. The W+jets contribution in the last bin of the bottom plots is described in section 7.2, while the contribution to other bins is based on simulated events. The uncertainty band in these four plots includes both the statistical and systematic uncertainties.

There is no excess of events over the SM expectation. These results are interpreted in the context of a simplified model of chargino pair production and decay, which is described in section 3 and corresponds to the left diagram in figure 1.

JHEP04(2017)018

	$e\tau_h$	$\mu\tau_h$	$\tau_h\tau_h$ SR1	$\tau_h\tau_h$ SR2
DY	$0.19 \pm 0.04 \pm 0.03$	$0.25 \pm 0.06 \pm 0.04$	$0.56 \pm 0.07 \pm 0.12$	$0.81 \pm 0.56 \pm 0.18$
tX, VV, hX	$0.03 \pm 0.03 \pm 0.02$	$0.19 \pm 0.09 \pm 0.09$	$0.19 \pm 0.03 \pm 0.09$	$0.75 \pm 0.35 \pm 0.38$
W+jets	$3.30^{+3.35}_{-3.30} \pm 0.56$	$8.15 \pm 4.59 \pm 1.53$	$0.70 \pm 0.21 \pm 0.55$	$4.36 \pm 1.05 \pm 1.63$
QCD multijet	—	—	$0.13 \pm 0.06 \pm 0.21$	$1.15 \pm 0.39 \pm 0.74$
SM total	$3.52 \pm 3.35 \pm 0.56$	$8.59 \pm 4.59 \pm 1.53$	$1.58 \pm 0.23 \pm 0.61$	$7.07 \pm 1.30 \pm 1.84$
Observed	3	5	1	2
SUSY(380, 1)	$2.14 \pm 0.08 \pm 0.38$	$2.16 \pm 0.08 \pm 0.39$	$4.10 \pm 0.10 \pm 0.90$	$1.10 \pm 0.05 \pm 0.27$
SUSY(240, 40)	$1.43 \pm 0.19 \pm 0.21$	$0.96 \pm 0.14 \pm 0.14$	$4.35 \pm 0.27 \pm 0.91$	$3.60 \pm 0.25 \pm 0.83$
SUSY(180, 60)	$0.12 \pm 0.04 \pm 0.02$	$0.04 \pm 0.02 \pm 0.01$	$0.73 \pm 0.11 \pm 0.17$	$2.36 \pm 0.17 \pm 0.54$

Table 7. Data yields and background predictions with uncertainties in the four signal regions of the search. The uncertainties are reported in two parts, the statistical and systematic uncertainties, respectively. The W+jets and QCD multijet main backgrounds are derived from data as described in section 7; the abbreviation "VV" refers to diboson events. The yields for three signal points representing the low, medium, and high Δm are also shown. SUSY(X, Y) stands for a SUSY signal with $m_{\widetilde{\chi}_1^\pm} = \mathrm{X}\,\mathrm{GeV}$ and $m_{\widetilde{\chi}_1^0} = \mathrm{Y}\,\mathrm{GeV}$.

A modified frequentist approach, known as the LHC-style $\mathrm{CL_s}$ criterion [65–67], is used to set limits on cross sections at a 95% confidence level (CL). The results on the excluded regions are shown in figure 5. Combining all four signal regions, the observed limits rule out $\widetilde{\chi}_1^\pm$ masses up to 420 GeV for a massless $\widetilde{\chi}_1^0$. This can be compared to the ATLAS limit of 345 GeV for a massless $\widetilde{\chi}_1^0$ [19]. It should be noted that the ATLAS results are based on the $\tau_h\tau_h$ channel alone. Figure 6 shows the results in the $\tau_h\tau_h$ channel, where the $\widetilde{\chi}_1^\pm$ masses are excluded up to 400 GeV for a massless $\widetilde{\chi}_1^0$. In the whole region, the observed limits are within one standard deviation of the expected limits.

The results are also interpreted to set limits on $\widetilde{\tau}\widetilde{\tau}$ production, which corresponds to the right diagram in figure 1. In this simplified model, two $\widetilde{\tau}$ particles are directly produced from the pp collision and decay promptly to two τ leptons and two neutralinos. The effect of the two $\ell\tau_h$ channels are found to be negligible and therefore are not considered. To calculate the production cross section, $\widetilde{\tau}$ is defined as the left-handed $\widetilde{\tau}$ gauge eigenstates [54]. Since the cross section for direct production of sleptons is lower, no point is excluded and a 95% CL upper limit is set on the cross section as a function of the $\widetilde{\tau}$ mass. Figure 7 displays the ratio of the obtained upper limit on the cross section and the cross section expected from SUSY (signal strength) versus the mass of the $\widetilde{\tau}$ particle, with the $\widetilde{\chi}_1^0$ mass set to 1 GeV . The observed limit is within one standard deviation of the expected limit. The best limit, which corresponds to the lowest signal strength, is obtained for $m_{\widetilde{\tau}} = 150\,\mathrm{GeV}$. The observed (expected) upper limit on the cross section at this mass is 43 (56) fb which is almost two times larger than the theoretical NLO prediction.

10 Summary

A search for SUSY in the $\tau\tau$ final state has been performed where the τ pair is produced in a cascade decay from the electroweak production of a chargino pair. The data analyzed were from pp collisions at $\sqrt{s} = 8\,\mathrm{TeV}$ collected by the CMS detector at the LHC corresponding

JHEP04(2017)018

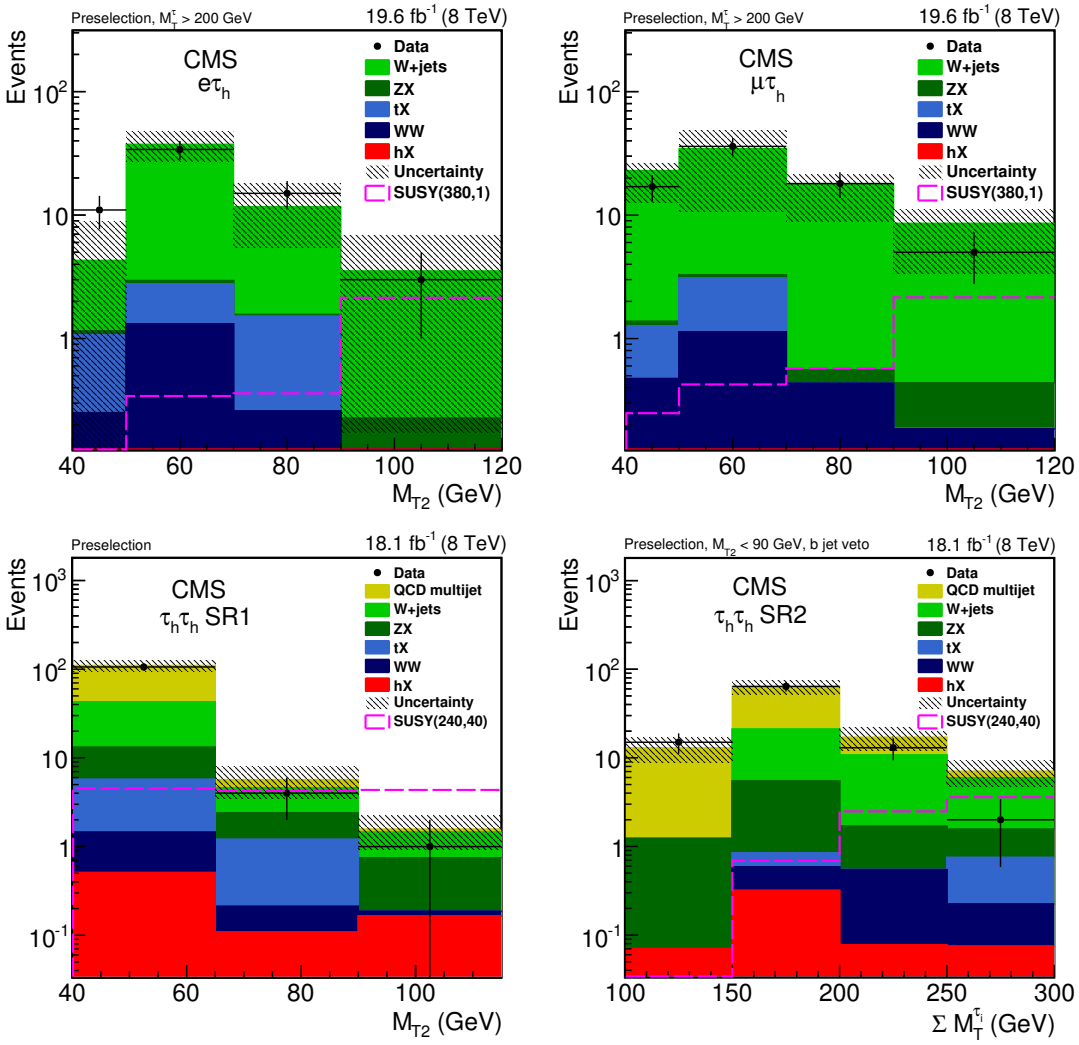

Figure 4. The data yield is compared with the SM expectation. In different signal regions, when a background estimate from data is available, it is used instead of simulation, as described in the text. The signal distribution for a high Δm scenario with $m_{\widetilde{\chi}_1^\pm} = 380\,\text{GeV}$ and $m_{\widetilde{\chi}_1^0} = 1\,\text{GeV}$ is compared with the yields of $\ell\tau_\text{h}$ channels while a scenario with lower Δm ($m_{\widetilde{\chi}_1^\pm} = 240\,\text{GeV}$ and $m_{\widetilde{\chi}_1^0} = 40\,\text{GeV}$) is chosen for the comparison in $\tau_\text{h}\tau_\text{h}$ channels. The higher values of M_{T2} or $\Sigma M_\text{T}^{\tau_i}$ are included in the last bins. The shown uncertainties include the quadratic sum of the statistical and systematic uncertainties.

to integrated luminosities between 18.1 and 19.6 fb^{-1}. To maximize the sensitivity, the selection criteria are optimized for $\tau_\text{h}\tau_\text{h}$ (small Δm), $\tau_\text{h}\tau_\text{h}$ (large Δm), and $\ell\tau_\text{h}$ channels using the variables M_{T2}, $M_\text{T}^{\tau_\text{h}}$, and $\Sigma M_\text{T}^{\tau_i}$. The observed number of events is consistent with the SM expectations. In the context of simplified models, assuming that the third generation sleptons are the lightest sleptons and that their masses lie midway between that of the chargino and the neutralino, charginos lighter than 420 GeV for a massless neutralino are excluded at a 95% confidence level. For neutralino masses up to 100 GeV, chargino masses up to 325 GeV are excluded at a 95% confidence level. Upper limits on

JHEP04(2017)018

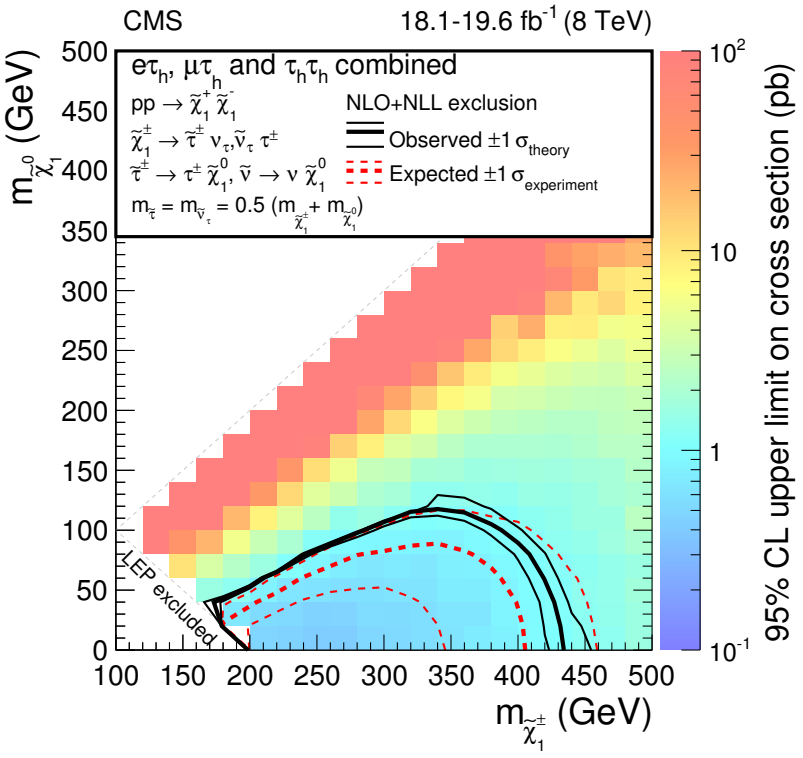

Figure 5. Expected and observed exclusion regions in terms of simplified models of chargino pair production with the total data set of 2012. The triangle in the bottom-left corner corresponds to $\tilde{\tau}$ masses below 96 GeV, which has been excluded by the LEP experiments [68]. The expected limits and the contours corresponding to ±1 standard deviation from experimental uncertainties are shown as red lines. The observed limits are shown with a black solid line, while the ±1 standard deviation based on the signal cross section uncertainties are shown with narrower black lines.

the direct $\tilde{\tau}\tilde{\tau}$ production cross section are also provided, and the best limit obtained is for the massless neutralino scenario, which is two times larger than the theoretical NLO cross sections.

Acknowledgments

We congratulate our colleagues in the CERN accelerator departments for the excellent performance of the LHC and thank the technical and administrative staffs at CERN and at other CMS institutes for their contributions to the success of the CMS effort. In addition, we gratefully acknowledge the computing centres and personnel of the Worldwide LHC Computing Grid for delivering so effectively the computing infrastructure essential to our analyses. Finally, we acknowledge the enduring support for the construction and operation of the LHC and the CMS detector provided by the following funding agencies: the Austrian Federal Ministry of Science, Research and Economy and the Austrian Science Fund; the Belgian Fonds de la Recherche Scientifique, and Fonds voor Wetenschappelijk Onderzoek; the Brazilian Funding Agencies (CNPq, CAPES, FAPERJ, and FAPESP); the Bulgarian

JHEP04(2017)018

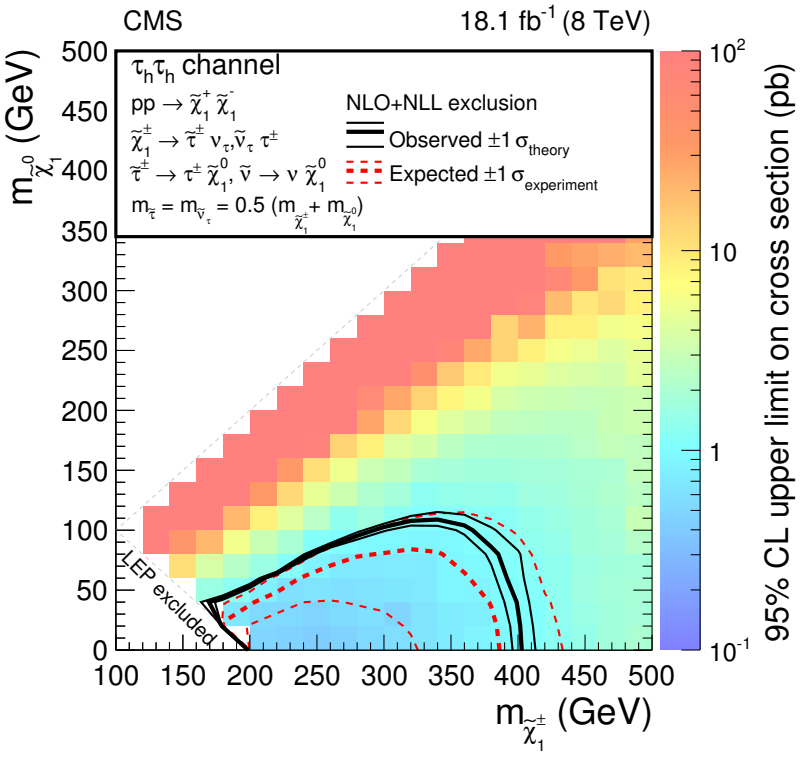

Figure 6. Expected and observed exclusion regions in terms of simplified models in the $\tau_h\tau_h$ channel. The conventions are the same as figure 5.

Ministry of Education and Science; CERN; the Chinese Academy of Sciences, Ministry of Science and Technology, and National Natural Science Foundation of China; the Colombian Funding Agency (COLCIENCIAS); the Croatian Ministry of Science, Education and Sport, and the Croatian Science Foundation; the Research Promotion Foundation, Cyprus; the Secretariat for Higher Education, Science, Technology and Innovation, Ecuador; the Ministry of Education and Research, Estonian Research Council via IUT23-4 and IUT23-6 and European Regional Development Fund, Estonia; the Academy of Finland, Finnish Ministry of Education and Culture, and Helsinki Institute of Physics; the Institut National de Physique Nucléaire et de Physique des Particules / CNRS, and Commissariat à l'Énergie Atomique et aux Énergies Alternatives / CEA, France; the Bundesministerium für Bildung und Forschung, Deutsche Forschungsgemeinschaft, and Helmholtz-Gemeinschaft Deutscher Forschungszentren, Germany; the General Secretariat for Research and Technology, Greece; the National Scientific Research Foundation, and National Innovation Office, Hungary; the Department of Atomic Energy and the Department of Science and Technology, India; the Institute for Studies in Theoretical Physics and Mathematics, Iran; the Science Foundation, Ireland; the Istituto Nazionale di Fisica Nucleare, Italy; the Ministry of Science, ICT and Future Planning, and National Research Foundation (NRF), Republic of Korea; the Lithuanian Academy of Sciences; the Ministry of Education, and University of Malaya (Malaysia); the Mexican Funding Agencies (BUAP, CINVESTAV, CONACYT, LNS, SEP,

JHEP04(2017)018

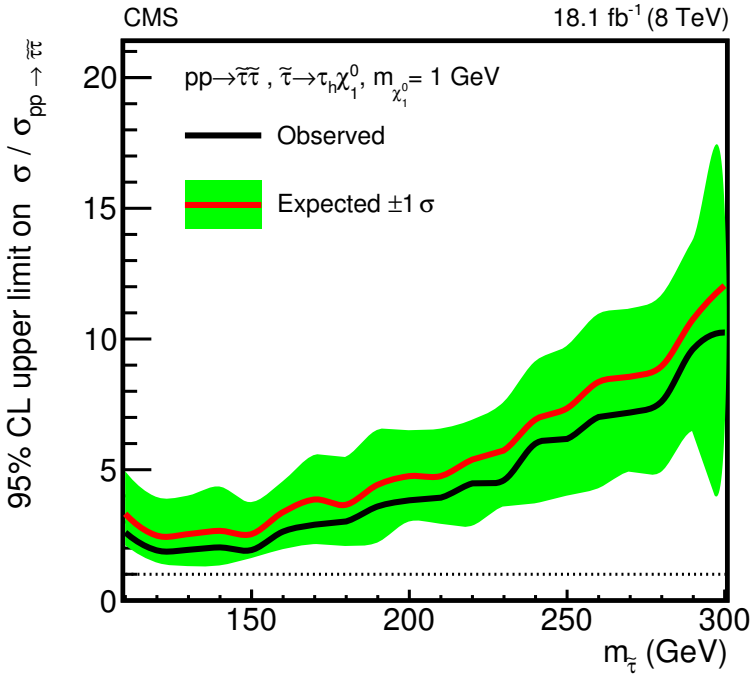

Figure 7. Upper limits at 95% confidence level on the left-handed $\tilde{\tau}$ pair production cross section in the $\tau_h\tau_h$ channel. The mass of $\tilde{\chi}_1^0$ is 1 GeV . The best observed (expected) upper limit on the cross section is 43 (56) fb for $m_{\tilde{\tau}} = 150$ GeV which is almost two times larger than the theoretical NLO prediction.

and UASLP-FAI); the Ministry of Business, Innovation and Employment, New Zealand; the Pakistan Atomic Energy Commission; the Ministry of Science and Higher Education and the National Science Centre, Poland; the Fundação para a Ciência e a Tecnologia, Portugal; JINR, Dubna; the Ministry of Education and Science of the Russian Federation, the Federal Agency of Atomic Energy of the Russian Federation, Russian Academy of Sciences, and the Russian Foundation for Basic Research; the Ministry of Education, Science and Technological Development of Serbia; the Secretaría de Estado de Investigación, Desarrollo e Innovación and Programa Consolider-Ingenio 2010, Spain; the Swiss Funding Agencies (ETH Board, ETH Zurich, PSI, SNF, UniZH, Canton Zurich, and SER); the Ministry of Science and Technology, Taipei; the Thailand Center of Excellence in Physics, the Institute for the Promotion of Teaching Science and Technology of Thailand, Special Task Force for Activating Research and the National Science and Technology Development Agency of Thailand; the Scientific and Technical Research Council of Turkey, and Turkish Atomic Energy Authority; the National Academy of Sciences of Ukraine, and State Fund for Fundamental Researches, Ukraine; the Science and Technology Facilities Council, U.K.; the US Department of Energy, and the US National Science Foundation.

Individuals have received support from the Marie-Curie programme and the European Research Council and EPLANET (European Union); the Leventis Foundation; the A. P. Sloan Foundation; the Alexander von Humboldt Foundation; the Belgian Federal Science Policy Office; the Fonds pour la Formation à la Recherche dans l'Industrie et dans

JHEP04(2017)018

l'Agriculture (FRIA-Belgium); the Agentschap voor Innovatie door Wetenschap en Technologie (IWT-Belgium); the Ministry of Education, Youth and Sports (MEYS) of the Czech Republic; the Council of Science and Industrial Research, India; the HOMING PLUS programme of the Foundation for Polish Science, cofinanced from European Union, Regional Development Fund, the Mobility Plus programme of the Ministry of Science and Higher Education, the OPUS programme contract 2014/13/B/ST2/02543 and contract Sonatabis DEC-2012/07/E/ST2/01406 of the National Science Center (Poland); the Thalis and Aristeia programmes cofinanced by EU-ESF and the Greek NSRF; the National Priorities Research Program by Qatar National Research Fund; the Programa Clarín-COFUND del Principado de Asturias; the Rachadapisek Sompot Fund for Postdoctoral Fellowship, Chulalongkorn University and the Chulalongkorn Academic into Its 2nd Century Project Advancement Project (Thailand); and the Welch Foundation, contract C-1845.

A Additional information for new model testing

In the previous sections, a simplified SUSY model is used to optimize the selection criteria and interpret the results. Here, the main efficiencies versus generated values are reported, so that these results can be used in an approximate manner to examine new models in a MC generator-level study. The number of the passed signal events and its uncertainty that can be evaluated by a generator-level study should be combined statistically with the results in table 7 to find the upper limit on the number of signal events and decide if a model is excluded or still allowed according to the analysis presented in this paper.

Efficiencies are provided as a function of the kinematic properties (e.g., p_{T}) of visible τ lepton decay products at the generator level. The visible τ lepton (τ_{vis}), if it decays leptonically, is defined as the 4-vector of the light charged lepton. In hadronic decays, τ_{vis} is the difference between the 4-vector of the τ lepton and neutrino in the hadronic decay. The visible τ objects are required to pass the offline kinematic selection criteria (η and p_{T} requirements). The $\not{p}_{\mathrm{T}}^{\mathrm{gen}}$ variable is defined as the magnitude of the negative vector sum of the τ_{vis} pairs in the transverse plane. The 4-vector of the τ_{vis} objects and $\not{p}_{\mathrm{T}}^{\mathrm{gen}}$ are used to calculate the M_{T} of the τ_{vis} objects and also the generator-level M_{T2}. All efficiencies are derived using the SUSY chargino pair production sample. The chargino mass is varied from 120 to 500 GeV and the neutralino mass from 1 to 500 GeV . Table 8 shows the efficiencies for selecting a lepton or τ_{h} for different channels versus p_{T} (τ_{vis}). These efficiencies include the scale factors, and efficiencies of object identification, isolation, and trigger. Table 9 shows the efficiencies in all channels to pass the $p_{\mathrm{T}}^{\mathrm{miss}} > 30$ GeV requirement as a function of the $\not{p}_{\mathrm{T}}^{\mathrm{gen}}$. Table 10 shows the efficiencies in different channels to pass the requirement of the reconstructed invariant mass versus the invariant mass of the τ_{vis} pair (generated mass). The requirements on the invariant mass of the reconstructed pair are (>15 GeV) and (<45 or >75 GeV) for the $\ell\tau_{\mathrm{h}}$ channels and (<55 or >85 GeV) for the $\tau_{\mathrm{h}}\tau_{\mathrm{h}}$ channel. The efficiencies of the ($M_{\mathrm{T2}} > 90$ GeV) requirement in $\ell\tau_{\mathrm{h}}$ signal region and $\tau_{\mathrm{h}}\tau_{\mathrm{h}}$ SR1 are listed in table 11. Table 12 shows the efficiencies in the $\ell\tau_{\mathrm{h}}$ channels to pass the $M_{\mathrm{T}}^{\tau_{\mathrm{h}}} > 200$ GeV requirement versus generated $M_{\mathrm{T}}^{\tau_{\mathrm{h}}}$.

JHEP04(2017)018

p_{T} (ℓ or τ_{vis}) (GeV)	e for eτ_{h}	μ for $\mu\tau_{\mathrm{h}}$	τ_{h} for $\ell\tau_{\mathrm{h}}$	τ_{h}^{1} for $\tau_{\mathrm{h}}\tau_{\mathrm{h}}$	τ_{h}^{2} for $\tau_{\mathrm{h}}\tau_{\mathrm{h}}$
20–30	0.27	0.80	0.20	0	0
30–40	0.68	0.86	0.36	0	0
40–60	0.75	0.87	0.42	0.04	0.61
60–80	0.80	0.89	0.47	0.14	0.69
80–120	0.83	0.90	0.50	0.26	0.70
120–160	0.86	0.90	0.51	0.31	0.70
160–200	0.87	0.91	0.51	0.34	0.71
>200	0.89	0.92	0.51	0.37	0.71

Table 8. Efficiencies to select a lepton or τ_{h} in different channels. Here, τ_{h}^{1} and τ_{h}^{2} stand for leading and subleading (in p_{T}) τ_{h} in the $\tau_{\mathrm{h}}\tau_{\mathrm{h}}$ channel. Zero for the efficiency shows the region where the generated τ leptons do not pass the kinematical and geometrical selection cuts.

$\not{p}_{\mathrm{T}}^{\mathrm{gen}}$ (GeV)	All channels
0–10	0.52
10–20	0.58
20–30	0.68
30–40	0.79
40–50	0.87
50–60	0.93
60–70	0.95
70–80	0.97
80–90	0.98
90–100	0.98
100–120	0.99
120–140	0.99
140–160	0.99
>160	1.00

Table 9. Efficiencies of the $p_{\mathrm{T}}^{\mathrm{miss}}$ requirement in all channels versus $\not{p}_{\mathrm{T}}^{\mathrm{gen}}$.

In the $\tau_{\mathrm{h}}\tau_{\mathrm{h}}$ SR2, the reconstructed M_{T2} is constrained to lie between 40 and 90 GeV. Table 13 shows the efficiencies in $\tau_{\mathrm{h}}\tau_{\mathrm{h}}$ SR2 to pass the $40 < M_{\mathrm{T2}} < 90$ GeV requirement versus generated M_{T2}. The last selection in this channel is the requirement on $\Sigma M_{\mathrm{T}}^{\tau_i}$, which is calculated using the 4-vector of the two τ_{vis} and $\not{p}_{\mathrm{T}}^{\mathrm{gen}}$. Table 14 shows the efficiencies in $\tau_{\mathrm{h}}\tau_{\mathrm{h}}$ SR2 to pass the $\Sigma M_{\mathrm{T}}^{\tau_i} > 250$ GeV requirement versus generated $\Sigma M_{\mathrm{T}}^{\tau_i}$.

To take into account the inefficiencies and misidentifications for charge reconstruction of the objects, identification of the b-tagged jets, identification of the extra leptons and the minimum angle between the jets and $E_{\mathrm{T}}^{\mathrm{miss}}$ in the transverse plane, the final yields in $\ell\tau_{\mathrm{h}}$ and $\tau_{\mathrm{h}}\tau_{\mathrm{h}}$ channels must be multiplied by 0.8 and 0.7, respectively.

To use these efficiencies, one needs to multiply the values one after another and combine statistically the final value with the values reported in table 7 statistically, to decide if a signal point is excluded. At the generator level, a pair of $\ell\tau_{\mathrm{h}}$ or $\tau_{\mathrm{h}}\tau_{\mathrm{h}}$ is selected, when the τ_{vis} objects pass the corresponding offline kinematic selection criteria.

JHEP04(2017)018

Generated mass (GeV)	$\ell\tau_h$	$\tau_h\tau_h$
5–10	0.10	0
10–15	0.23	0.20
15–20	0.97	0.90
20–25	0.99	0.94
25–30	1.00	0.98
30–35	0.99	1.00
35–40	0.98	1.00
40–45	0.84	0.99
45–50	0.16	0.95
50–55	0.04	0.68
55–60	0.02	0.18
60–65	0.01	0.06
65–70	0.04	0.03
70–75	0.23	0.05
75–80	0.78	0.15
80–85	0.91	0.40
85–90	0.96	0.78
90–95	0.97	0.92
95–100	0.98	0.95
100–105	1.00	0.98
105–110	1.00	0.99
>110	1.00	1.00

Table 10. Efficiencies of the invariant mass requirements in different channels versus generated mass.

Generated M_{T2} (GeV)	$\ell\tau_h$	$\tau_h\tau_h$ SR1
20–40	0.002	0.01
40–50	0.01	0.01
50–60	0.02	0.03
60–70	0.05	0.07
70–80	0.13	0.17
80–90	0.35	0.44
90–100	0.65	0.73
100–110	0.82	0.88
110–120	0.90	0.94
120–130	0.93	0.97
130–140	0.95	0.98
140–160	0.96	0.98
160–180	0.97	0.99
>180	0.97	1.00

Table 11. Efficiencies of the $M_{T2} > 90\,\text{GeV}$ requirement in all channels versus generated M_{T2}.

JHEP04(2017)018

Generated $M_{\mathrm{T}}^{\tau_{\mathrm{h}}}$ (GeV)	$\ell\tau_{\mathrm{h}}$
100–125	0.01
125–150	0.03
150–170	0.09
170–190	0.26
190–200	0.51
200–210	0.67
210–230	0.82
230–250	0.91
250–275	0.94
275–300	0.97
>300	1.00

Table 12. Efficiencies of the $M_{\mathrm{T}}^{\tau_{\mathrm{h}}}$ requirement in $\ell\tau_{\mathrm{h}}$ channels versus generated $M_{\mathrm{T}}^{\tau_{\mathrm{h}}}$.

Generated M_{T2} (GeV)	$\tau_{\mathrm{h}}\tau_{\mathrm{h}}$ SR2
0–20	0.08
20–40	0.43
40–50	0.75
50–60	0.82
60–70	0.81
70–80	0.72
80–90	0.49
90–100	0.24
100–110	0.11
110–120	0.05
120–130	0.03
130–140	0.02
140–160	0.01
160–180	0.01
>180	0

Table 13. Efficiencies of the M_{T2} requirement in $\tau_{\mathrm{h}}\tau_{\mathrm{h}}$ SR2 versus generated M_{T2}. Zero for the efficiency shows the region that the generated M_{T2} is much greater than the selection cut.

The efficiencies are used to reproduce the yields in the SMS plane. The results are in agreement with the yields from the full chain of simulation and reconstruction within ∼30%. A user of these efficiencies should be aware that some assumptions can be broken close to the diagonal (very low mass difference between chargino and neutralino) and these efficiencies cannot be used. This compressed region requires a separate analysis, because the mass difference of the parent particle and its decay products is comparable to the energy threshold used in this analysis to select the objects.

JHEP04(2017)018

Generated $\Sigma M_{\mathrm{T}}^{\tau_i}$ (GeV)	$\tau_{\mathrm{h}}\tau_{\mathrm{h}}$ SR2
80–180	0.16
180–200	0.19
200–210	0.25
210–220	0.30
220–230	0.36
230–240	0.43
240–250	0.52
250–260	0.55
260–270	0.61
270–280	0.67
280–290	0.68
290–300	0.73
300–320	0.76
320–340	0.77
340–360	0.80
360–380	0.81
380–400	0.81
>400	0.82

Table 14. Efficiencies of the $\Sigma M_{\mathrm{T}}^{\tau_i}$ requirement in $\tau_{\mathrm{h}}\tau_{\mathrm{h}}$ SR2 versus the generated $\Sigma M_{\mathrm{T}}^{\tau_i}$.

Open Access. This article is distributed under the terms of the Creative Commons Attribution License (CC-BY 4.0), which permits any use, distribution and reproduction in any medium, provided the original author(s) and source are credited.

References

[1] Y.A. Golfand and E.P. Likhtman, *Extension of the algebra of Poincare group generators and violation of P invariance*, *JETP. Lett.* **13** (1971) 323.

[2] J. Wess and B. Zumino, *A Lagrangian Model Invariant Under Supergauge Transformations*, *Phys. Lett.* **49B** (1974) 52 [INSPIRE].

[3] J. Wess and B. Zumino, *Supergauge Transformations in Four-Dimensions*, *Nucl. Phys.* **B 70** (1974) 39 [INSPIRE].

[4] P. Fayet, *Spontaneously Broken Supersymmetric Theories of Weak, Electromagnetic and Strong Interactions*, *Phys. Lett.* **B 69** (1977) 489 [INSPIRE].

[5] G.R. Farrar and P. Fayet, *Phenomenology of the Production, Decay and Detection of New Hadronic States Associated with Supersymmetry*, *Phys. Lett.* **76B** (1978) 575 [INSPIRE].

[6] CMS collaboration, *Search for new physics in events with same-sign dileptons and jets in pp collisions at* $\sqrt{s} = 8$ *TeV*, *JHEP* **01** (2014) 163 [*Erratum ibid.* **1501** (2015) 014] [arXiv:1311.6736] [INSPIRE].

JHEP04(2017)018

[7] CMS collaboration, *Search for supersymmetry in hadronic final states with missing transverse energy using the variables α_T and b-quark multiplicity in pp collisions at $\sqrt{s} = 8$ TeV*, *Eur. Phys. J.* **C 73** (2013) 2568 [arXiv:1303.2985] [INSPIRE].

[8] CMS collaboration, *Search for anomalous production of events with three or more leptons in pp collisions at $\sqrt{s} = 8$ TeV*, *Phys. Rev.* **D 90** (2014) 032006 [arXiv:1404.5801] [INSPIRE].

[9] CMS collaboration, *Search for new physics in the multijet and missing transverse momentum final state in proton-proton collisions at $\sqrt{s} = 8$ TeV*, *JHEP* **06** (2014) 055 [arXiv:1402.4770] [INSPIRE].

[10] CMS collaboration, *Searches for Supersymmetry using the M_{T2} Variable in Hadronic Events Produced in pp Collisions at 8 TeV*, *JHEP* **05** (2015) 078 [arXiv:1502.04358] [INSPIRE].

[11] CMS collaboration, *Search for Physics Beyond the Standard Model in Events with Two Leptons, Jets and Missing Transverse Momentum in pp Collisions at $\sqrt{s} = 8$ TeV*, *JHEP* **04** (2015) 124 [arXiv:1502.06031] [INSPIRE].

[12] ATLAS collaboration, *ATLAS Run 1 searches for direct pair production of third-generation squarks at the Large Hadron Collider*, *Eur. Phys. J.* **C 75** (2015) 510 [arXiv:1506.08616] [INSPIRE].

[13] ATLAS collaboration, *Summary of the searches for squarks and gluinos using $\sqrt{s} = 8$ TeV pp collisions with the ATLAS experiment at the LHC*, *JHEP* **10** (2015) 054 [arXiv:1507.05525] [INSPIRE].

[14] ATLAS collaboration, *Search for direct production of charginos and neutralinos in events with three leptons and missing transverse momentum in $\sqrt{s} = 8$ TeV pp collisions with the ATLAS detector*, *JHEP* **04** (2014) 169 [arXiv:1402.7029] [INSPIRE].

[15] ATLAS collaboration, *Search for direct production of charginos, neutralinos and sleptons in final states with two leptons and missing transverse momentum in pp collisions at $\sqrt{s} = 8$ TeV with the ATLAS detector*, *JHEP* **05** (2014) 071 [arXiv:1403.5294] [INSPIRE].

[16] CMS collaboration, *Searches for electroweak production of charginos, neutralinos and sleptons decaying to leptons and W, Z and Higgs bosons in pp collisions at 8 TeV*, *Eur. Phys. J.* **C 74** (2014) 3036 [arXiv:1405.7570] [INSPIRE].

[17] CMS collaboration, *Searches for electroweak neutralino and chargino production in channels with Higgs, Z and W bosons in pp collisions at 8 TeV*, *Phys. Rev.* **D 90** (2014) 092007 [arXiv:1409.3168] [INSPIRE].

[18] CMS collaboration, *Search for supersymmetry in the vector-boson fusion topology in proton-proton collisions at $\sqrt{s} = 8$ TeV*, *JHEP* **11** (2015) 189 [arXiv:1508.07628] [INSPIRE].

[19] ATLAS collaboration, *Search for the direct production of charginos, neutralinos and staus in final states with at least two hadronically decaying taus and missing transverse momentum in pp collisions at $\sqrt{s} = 8$ TeV with the ATLAS detector*, *JHEP* **10** (2014) 096 [arXiv:1407.0350] [INSPIRE].

[20] ATLAS collaboration, *Search for the electroweak production of supersymmetric particles in $\sqrt{s} = 8$ TeV pp collisions with the ATLAS detector*, *Phys. Rev.* **D 93** (2016) 052002 [arXiv:1509.07152] [INSPIRE].

[21] S.P. Martin, *A Supersymmetry primer*, hep-ph/9709356 [INSPIRE].

[22] J. Alwall, P. Schuster and N. Toro, *Simplified Models for a First Characterization of New Physics at the LHC*, *Phys. Rev.* **D 79** (2009) 075020 [arXiv:0810.3921] [INSPIRE].

JHEP04(2017)018

[23] LHC New Physics Working Group collaboration, D. Alves, *Simplified Models for LHC New Physics Searches*, *J. Phys.* **G 39** (2012) 105005 [arXiv:1105.2838] [INSPIRE].

[24] C.G. Lester and D.J. Summers, *Measuring masses of semiinvisibly decaying particles pair produced at hadron colliders*, *Phys. Lett.* **B 463** (1999) 99 [hep-ph/9906349] [INSPIRE].

[25] A. Barr, C. Lester and P. Stephens, *m(T2): The Truth behind the glamour*, *J. Phys.* **G 29** (2003) 2343 [hep-ph/0304226] [INSPIRE].

[26] CMS collaboration, *The CMS Experiment at the CERN LHC*, 2008 *JINST* **3** S08004 [INSPIRE].

[27] CMS collaboration, *The CMS trigger system*, 2017 *JINST* **12** P01020 [arXiv:1609.02366] [INSPIRE].

[28] CMS collaboration, *Particle-Flow Event Reconstruction in CMS and Performance for Jets, Taus and MET*, CMS-PAS-PFT-09-001.

[29] CMS collaboration, *Commissioning of the Particle-flow Event Reconstruction with the first LHC collisions recorded in the CMS detector*, CMS-PAS-PFT-10-001.

[30] M. Cacciari, G.P. Salam and G. Soyez, *The Anti-k(t) jet clustering algorithm*, *JHEP* **04** (2008) 063 [arXiv:0802.1189] [INSPIRE].

[31] CMS collaboration, *Determination of Jet Energy Calibration and Transverse Momentum Resolution in CMS*, 2011 *JINST* **6** P11002 [arXiv:1107.4277] [INSPIRE].

[32] M. Cacciari and G.P. Salam, *Pileup subtraction using jet areas*, *Phys. Lett.* **B 659** (2008) 119 [arXiv:0707.1378] [INSPIRE].

[33] CMS collaboration, *Identification of b-quark jets with the CMS experiment*, 2013 *JINST* **8** P04013 [arXiv:1211.4462] [INSPIRE].

[34] CMS collaboration, *Reconstruction and identification of τ lepton decays to hadrons and ν_τ at CMS*, 2016 *JINST* **11** P01019 [arXiv:1510.07488] [INSPIRE].

[35] CMS collaboration, *Search for neutral MSSM Higgs bosons decaying to a pair of tau leptons in pp collisions*, *JHEP* **10** (2014) 160 [arXiv:1408.3316] [INSPIRE].

[36] P.M. Nadolsky et al., *Implications of CTEQ global analysis for collider observables*, *Phys. Rev.* **D 78** (2008) 013004 [arXiv:0802.0007] [INSPIRE].

[37] T. Sjöstrand, S. Mrenna and P.Z. Skands, *PYTHIA 6.4 Physics and Manual*, *JHEP* **05** (2006) 026 [hep-ph/0603175] [INSPIRE].

[38] J. Alwall, M. Herquet, F. Maltoni, O. Mattelaer and T. Stelzer, *MadGraph 5: Going Beyond*, *JHEP* **06** (2011) 128 [arXiv:1106.0522] [INSPIRE].

[39] P. Nason, *A New method for combining NLO QCD with shower Monte Carlo algorithms*, *JHEP* **11** (2004) 040 [hep-ph/0409146] [INSPIRE].

[40] S. Frixione, P. Nason and C. Oleari, *Matching NLO QCD computations with Parton Shower simulations: the POWHEG method*, *JHEP* **11** (2007) 070 [arXiv:0709.2092] [INSPIRE].

[41] S. Alioli, P. Nason, C. Oleari and E. Re, *NLO single-top production matched with shower in POWHEG: s- and t-channel contributions*, *JHEP* **09** (2009) 111 [*Erratum ibid.* **1002** (2010) 011] [arXiv:0907.4076] [INSPIRE].

JHEP04(2017)018

[42] S. Alioli, P. Nason, C. Oleari and E. Re, *A general framework for implementing NLO calculations in shower Monte Carlo programs: the POWHEG BOX*, *JHEP* **06** (2010) 043 [arXiv:1002.2581] [INSPIRE].

[43] CMS collaboration, *Measurement of the top quark mass using proton-proton data at* $\sqrt{(s)} = 7$ *and 8 TeV*, *Phys. Rev.* **D 93** (2016) 072004 [arXiv:1509.04044] [INSPIRE].

[44] ATLAS, CMS collaboration, *Combined Measurement of the Higgs Boson Mass in pp Collisions at* $\sqrt{s} = 7$ *and 8 TeV with the ATLAS and CMS Experiments*, *Phys. Rev. Lett.* **114** (2015) 191803 [arXiv:1503.07589] [INSPIRE].

[45] N. Davidson, G. Nanava, T. Przedzinski, E. Richter-Was and Z. Was, *Universal Interface of TAUOLA Technical and Physics Documentation*, *Comput. Phys. Commun.* **183** (2012) 821 [arXiv:1002.0543] [INSPIRE].

[46] GEANT4 collaboration, S. Agostinelli et al., *GEANT4: A Simulation toolkit*, *Nucl. Instrum. Meth.* **A 506** (2003) 250 [INSPIRE].

[47] CMS collaboration, S. Abdullin, P. Azzi, F. Beaudette, P. Janot and A. Perrotta, *The fast simulation of the CMS detector at LHC*, *J. Phys. Conf. Ser.* **331** (2011) 032049 [INSPIRE].

[48] K. Melnikov and F. Petriello, *Electroweak gauge boson production at hadron colliders through* $O(\alpha_s^2)$, *Phys. Rev.* **D 74** (2006) 114017 [hep-ph/0609070] [INSPIRE].

[49] R. Gavin, Y. Li, F. Petriello and S. Quackenbush, *W Physics at the LHC with FEWZ 2.1*, *Comput. Phys. Commun.* **184** (2013) 208 [arXiv:1201.5896] [INSPIRE].

[50] M. Czakon and A. Mitov, *Top++: A Program for the Calculation of the Top-Pair Cross-Section at Hadron Colliders*, *Comput. Phys. Commun.* **185** (2014) 2930 [arXiv:1112.5675] [INSPIRE].

[51] J.M. Campbell, R.K. Ellis and C. Williams, *Vector boson pair production at the LHC*, *JHEP* **07** (2011) 018 [arXiv:1105.0020] [INSPIRE].

[52] B. Fuks, M. Klasen, D.R. Lamprea and M. Rothering, *Gaugino production in proton-proton collisions at a center-of-mass energy of 8 TeV*, *JHEP* **10** (2012) 081 [arXiv:1207.2159] [INSPIRE].

[53] B. Fuks, M. Klasen, D.R. Lamprea and M. Rothering, *Precision predictions for electroweak superpartner production at hadron colliders with Resummino*, *Eur. Phys. J.* **C 73** (2013) 2480 [arXiv:1304.0790] [INSPIRE].

[54] B. Fuks, M. Klasen, D.R. Lamprea and M. Rothering, *Revisiting slepton pair production at the Large Hadron Collider*, *JHEP* **01** (2014) 168 [arXiv:1310.2621] [INSPIRE].

[55] A.J. Barr and C. Gwenlan, *The Race for supersymmetry: Using m(T2) for discovery*, *Phys. Rev.* **D 80** (2009) 074007 [arXiv:0907.2713] [INSPIRE].

[56] CDF collaboration, T. Affolder et al., *Measurement of the W boson mass with the Collider Detector at Fermilab*, *Phys. Rev.* **D 64** (2001) 052001 [hep-ex/0007044] [INSPIRE].

[57] D0 collaboration, V.M. Abazov et al., *Improved W boson mass measurement with the DØ detector*, *Phys. Rev.* **D 66** (2002) 012001 [hep-ex/0204014] [INSPIRE].

[58] CMS collaboration, *Measurement of the Inclusive Z Cross Section via Decays to Tau Pairs in pp Collisions at* $\sqrt{s} = 7$ *TeV*, *JHEP* **08** (2011) 117 [arXiv:1104.1617] [INSPIRE].

JHEP04(2017)018

[59] CMS collaboration, *Performance of Electron Reconstruction and Selection with the CMS Detector in Proton-Proton Collisions at* $\sqrt{s} = 8$ *TeV*, 2015 *JINST* **10** P06005 [arXiv:1502.02701] [INSPIRE].

[60] CMS collaboration, *Performance of CMS muon reconstruction in pp collision events at* $\sqrt{s} = 7$ *TeV*, 2012 *JINST* **7** P10002 [arXiv:1206.4071] [INSPIRE].

[61] CMS collaboration, *Measurement of inclusive W and Z boson production cross sections in pp collisions at* $\sqrt{s} = 8$ *TeV*, *Phys. Rev. Lett.* **112** (2014) 191802 [arXiv:1402.0923] [INSPIRE].

[62] G. Antchev et al., *First measurement of the total proton-proton cross section at the LHC energy of* $\sqrt{s} = 7$ *TeV*, *Europhys. Lett.* **96** (2011) 21002 [arXiv:1110.1395] [INSPIRE].

[63] TOTEM collaboration, M. Botje et al., *The PDF4LHC Working Group Interim Recommendations*, arXiv:1101.0538 [INSPIRE].

[64] CMS collaboration, *CMS Luminosity Based on Pixel Cluster Counting — Summer 2013 Update*, CMS-PAS-LUM-13-001.

[65] A.L. Read, *Presentation of search results: The* CL_s *technique*, *J. Phys.* **G 28** (2002) 2693 [INSPIRE].

[66] T. Junk, *Confidence level computation for combining searches with small statistics*, *Nucl. Instrum. Meth.* **A 434** (1999) 435 [hep-ex/9902006] [INSPIRE].

[67] ATLAS collaboration, *Procedure for the LHC Higgs boson search combination in summer 2011*, ATL-PHYS-PUB-2011-011 (2011).

[68] LEPSUSYWG, ALEPH, DELPHI, L3 and OPAL experiments, note LEPSUSYWG/04-01.1 (2004).

JHEP04(2017)018

The CMS collaboration

Yerevan Physics Institute, Yerevan, Armenia

V. Khachatryan, A.M. Sirunyan, A. Tumasyan

Institut für Hochenergiephysik, Wien, Austria

W. Adam, E. Asilar, T. Bergauer, J. Brandstetter, E. Brondolin, M. Dragicevic, J. Erö, M. Flechl, M. Friedl, R. Frühwirth[1], V.M. Ghete, C. Hartl, N. Hörmann, J. Hrubec, M. Jeitler[1], A. König, I. Krätschmer, D. Liko, T. Matsushita, I. Mikulec, D. Rabady, N. Rad, B. Rahbaran, H. Rohringer, J. Schieck[1], J. Strauss, W. Treberer-Treberspurg, W. Waltenberger, C.-E. Wulz[1]

National Centre for Particle and High Energy Physics, Minsk, Belarus

V. Mossolov, N. Shumeiko, J. Suarez Gonzalez

Universiteit Antwerpen, Antwerpen, Belgium

S. Alderweireldt, E.A. De Wolf, X. Janssen, J. Lauwers, M. Van De Klundert, H. Van Haevermaet, P. Van Mechelen, N. Van Remortel, A. Van Spilbeeck

Vrije Universiteit Brussel, Brussel, Belgium

S. Abu Zeid, F. Blekman, J. D'Hondt, N. Daci, I. De Bruyn, K. Deroover, N. Heracleous, S. Lowette, S. Moortgat, L. Moreels, A. Olbrechts, Q. Python, S. Tavernier, W. Van Doninck, P. Van Mulders, I. Van Parijs

Université Libre de Bruxelles, Bruxelles, Belgium

H. Brun, C. Caillol, B. Clerbaux, G. De Lentdecker, H. Delannoy, G. Fasanella, L. Favart, R. Goldouzian, A. Grebenyuk, G. Karapostoli, T. Lenzi, A. Léonard, J. Luetic, T. Maerschalk, A. Marinov, A. Randle-conde, T. Seva, C. Vander Velde, P. Vanlaer, R. Yonamine, F. Zenoni, F. Zhang[2]

Ghent University, Ghent, Belgium

A. Cimmino, T. Cornelis, D. Dobur, A. Fagot, G. Garcia, M. Gul, D. Poyraz, S. Salva, R. Schöfbeck, A. Sharma, M. Tytgat, W. Van Driessche, E. Yazgan, N. Zaganidis

Université Catholique de Louvain, Louvain-la-Neuve, Belgium

H. Bakhshiansohi, C. Beluffi[3], O. Bondu, S. Brochet, G. Bruno, A. Caudron, S. De Visscher, C. Delaere, M. Delcourt, B. Francois, A. Giammanco, A. Jafari, P. Jez, M. Komm, V. Lemaitre, A. Magitteri, A. Mertens, M. Musich, C. Nuttens, K. Piotrzkowski, L. Quertenmont, M. Selvaggi, M. Vidal Marono, S. Wertz

Université de Mons, Mons, Belgium

N. Beliy

Centro Brasileiro de Pesquisas Fisicas, Rio de Janeiro, Brazil

W.L. Aldá Júnior, F.L. Alves, G.A. Alves, L. Brito, C. Hensel, A. Moraes, M.E. Pol, P. Rebello Teles

JHEP04(2017)018

Universidade do Estado do Rio de Janeiro, Rio de Janeiro, Brazil
E. Belchior Batista Das Chagas, W. Carvalho, J. Chinellato[4], A. Custódio, E.M. Da Costa, G.G. Da Silveira[5], D. De Jesus Damiao, C. De Oliveira Martins, S. Fonseca De Souza, L.M. Huertas Guativa, H. Malbouisson, D. Matos Figueiredo, C. Mora Herrera, L. Mundim, H. Nogima, W.L. Prado Da Silva, A. Santoro, A. Sznajder, E.J. Tonelli Manganote[4], A. Vilela Pereira

Universidade Estadual Paulista [a], Universidade Federal do ABC [b], São Paulo, Brazil
S. Ahuja[a], C.A. Bernardes[b], S. Dogra[a], T.R. Fernandez Perez Tomei[a], E.M. Gregores[b], P.G. Mercadante[b], C.S. Moon[a], S.F. Novaes[a], Sandra S. Padula[a], D. Romero Abad[b], J.C. Ruiz Vargas

Institute for Nuclear Research and Nuclear Energy, Sofia, Bulgaria
A. Aleksandrov, R. Hadjiiska, P. Iaydjiev, M. Rodozov, S. Stoykova, G. Sultanov, M. Vutova

University of Sofia, Sofia, Bulgaria
A. Dimitrov, I. Glushkov, L. Litov, B. Pavlov, P. Petkov

Beihang University, Beijing, China
W. Fang[6]

Institute of High Energy Physics, Beijing, China
M. Ahmad, J.G. Bian, G.M. Chen, H.S. Chen, M. Chen, Y. Chen[7], T. Cheng, C.H. Jiang, D. Leggat, Z. Liu, F. Romeo, S.M. Shaheen, A. Spiezia, J. Tao, C. Wang, Z. Wang, H. Zhang, J. Zhao

State Key Laboratory of Nuclear Physics and Technology, Peking University, Beijing, China
Y. Ban, G. Chen, Q. Li, S. Liu, Y. Mao, S.J. Qian, D. Wang, Z. Xu

Universidad de Los Andes, Bogota, Colombia
C. Avila, A. Cabrera, L.F. Chaparro Sierra, C. Florez, J.P. Gomez, C.F. González Hernández, J.D. Ruiz Alvarez, J.C. Sanabria

University of Split, Faculty of Electrical Engineering, Mechanical Engineering and Naval Architecture, Split, Croatia
N. Godinovic, D. Lelas, I. Puljak, P.M. Ribeiro Cipriano, T. Sculac

University of Split, Faculty of Science, Split, Croatia
Z. Antunovic, M. Kovac

Institute Rudjer Boskovic, Zagreb, Croatia
V. Brigljevic, D. Ferencek, K. Kadija, S. Micanovic, L. Sudic, T. Susa

University of Cyprus, Nicosia, Cyprus
A. Attikis, G. Mavromanolakis, J. Mousa, C. Nicolaou, F. Ptochos, P.A. Razis, H. Rykaczewski

JHEP04(2017)018

Charles University, Prague, Czech Republic
M. Finger[8], M. Finger Jr.[8]

Universidad San Francisco de Quito, Quito, Ecuador
E. Carrera Jarrin

Academy of Scientific Research and Technology of the Arab Republic of Egypt, Egyptian Network of High Energy Physics, Cairo, Egypt
A. Ellithi Kamel[9], M.A. Mahmoud[10,11], A. Radi[11,12]

National Institute of Chemical Physics and Biophysics, Tallinn, Estonia
B. Calpas, M. Kadastik, M. Murumaa, L. Perrini, M. Raidal, A. Tiko, C. Veelken

Department of Physics, University of Helsinki, Helsinki, Finland
P. Eerola, J. Pekkanen, M. Voutilainen

Helsinki Institute of Physics, Helsinki, Finland
J. Härkönen, V. Karimäki, R. Kinnunen, T. Lampén, K. Lassila-Perini, S. Lehti, T. Lindén, P. Luukka, J. Tuominiemi, E. Tuovinen, L. Wendland

Lappeenranta University of Technology, Lappeenranta, Finland
J. Talvitie, T. Tuuva

IRFU, CEA, Université Paris-Saclay, Gif-sur-Yvette, France
M. Besancon, F. Couderc, M. Dejardin, D. Denegri, B. Fabbro, J.L. Faure, C. Favaro, F. Ferri, S. Ganjour, S. Ghosh, A. Givernaud, P. Gras, G. Hamel de Monchenault, P. Jarry, I. Kucher, E. Locci, M. Machet, J. Malcles, J. Rander, A. Rosowsky, M. Titov, A. Zghiche

Laboratoire Leprince-Ringuet, Ecole Polytechnique, IN2P3-CNRS, Palaiseau, France
A. Abdulsalam, I. Antropov, S. Baffioni, F. Beaudette, P. Busson, L. Cadamuro, E. Chapon, C. Charlot, O. Davignon, R. Granier de Cassagnac, M. Jo, S. Lisniak, P. Miné, M. Nguyen, C. Ochando, G. Ortona, P. Paganini, P. Pigard, S. Regnard, R. Salerno, Y. Sirois, T. Strebler, Y. Yilmaz, A. Zabi

Institut Pluridisciplinaire Hubert Curien, Université de Strasbourg, Université de Haute Alsace Mulhouse, CNRS/IN2P3, Strasbourg, France
J.-L. Agram[13], J. Andrea, A. Aubin, D. Bloch, J.-M. Brom, M. Buttignol, E.C. Chabert, N. Chanon, C. Collard, E. Conte[13], X. Coubez, J.-C. Fontaine[13], D. Gelé, U. Goerlach, A.-C. Le Bihan, K. Skovpen, P. Van Hove

Centre de Calcul de l'Institut National de Physique Nucleaire et de Physique des Particules, CNRS/IN2P3, Villeurbanne, France
S. Gadrat

Université de Lyon, Université Claude Bernard Lyon 1, CNRS-IN2P3, Institut de Physique Nucléaire de Lyon, Villeurbanne, France
S. Beauceron, C. Bernet, G. Boudoul, E. Bouvier, C.A. Carrillo Montoya, R. Chierici, D. Contardo, B. Courbon, P. Depasse, H. El Mamouni, J. Fan, J. Fay, S. Gascon,

JHEP04(2017)018

M. Gouzevitch, G. Grenier, B. Ille, F. Lagarde, I.B. Laktineh, M. Lethuillier, L. Mirabito, A.L. Pequegnot, S. Perries, A. Popov[14], D. Sabes, V. Sordini, M. Vander Donckt, P. Verdier, S. Viret

Georgian Technical University, Tbilisi, Georgia

T. Toriashvili[15]

Tbilisi State University, Tbilisi, Georgia

Z. Tsamalaidze[8]

RWTH Aachen University, I. Physikalisches Institut, Aachen, Germany

C. Autermann, S. Beranek, L. Feld, A. Heister, M.K. Kiesel, K. Klein, M. Lipinski, A. Ostapchuk, M. Preuten, F. Raupach, S. Schael, C. Schomakers, J.F. Schulte, J. Schulz, T. Verlage, H. Weber, V. Zhukov[14]

RWTH Aachen University, III. Physikalisches Institut A, Aachen, Germany

M. Brodski, E. Dietz-Laursonn, D. Duchardt, M. Endres, M. Erdmann, S. Erdweg, T. Esch, R. Fischer, A. Güth, M. Hamer, T. Hebbeker, C. Heidemann, K. Hoepfner, S. Knutzen, M. Merschmeyer, A. Meyer, P. Millet, S. Mukherjee, M. Olschewski, K. Padeken, T. Pook, M. Radziej, H. Reithler, M. Rieger, F. Scheuch, L. Sonnenschein, D. Teyssier, S. Thüer

RWTH Aachen University, III. Physikalisches Institut B, Aachen, Germany

V. Cherepanov, G. Flügge, W. Haj Ahmad, F. Hoehle, B. Kargoll, T. Kress, A. Künsken, J. Lingemann, T. Müller, A. Nehrkorn, A. Nowack, I.M. Nugent, C. Pistone, O. Pooth, A. Stahl[16]

Deutsches Elektronen-Synchrotron, Hamburg, Germany

M. Aldaya Martin, C. Asawatangtrakuldee, K. Beernaert, O. Behnke, U. Behrens, A.A. Bin Anuar, K. Borras[17], A. Campbell, P. Connor, C. Contreras-Campana, F. Costanza, C. Diez Pardos, G. Dolinska, G. Eckerlin, D. Eckstein, E. Eren, E. Gallo[18], J. Garay Garcia, A. Geiser, A. Gizhko, J.M. Grados Luyando, P. Gunnellini, A. Harb, J. Hauk, M. Hempel[19], H. Jung, A. Kalogeropoulos, O. Karacheban[19], M. Kasemann, J. Keaveney, C. Kleinwort, I. Korol, D. Krücker, W. Lange, A. Lelek, J. Leonard, K. Lipka, A. Lobanov, W. Lohmann[19], R. Mankel, I.-A. Melzer-Pellmann, A.B. Meyer, G. Mittag, J. Mnich, A. Mussgiller, E. Ntomari, D. Pitzl, R. Placakyte, A. Raspereza, B. Roland, M.Ö. Sahin, P. Saxena, T. Schoerner-Sadenius, C. Seitz, S. Spannagel, N. Stefaniuk, G.P. Van Onsem, R. Walsh, C. Wissing

University of Hamburg, Hamburg, Germany

V. Blobel, M. Centis Vignali, A.R. Draeger, T. Dreyer, E. Garutti, D. Gonzalez, J. Haller, M. Hoffmann, A. Junkes, R. Klanner, R. Kogler, N. Kovalchuk, T. Lapsien, T. Lenz, I. Marchesini, D. Marconi, M. Meyer, M. Niedziela, D. Nowatschin, F. Pantaleo[16], T. Peiffer, A. Perieanu, J. Poehlsen, C. Sander, C. Scharf, P. Schleper, A. Schmidt, S. Schumann, J. Schwandt, H. Stadie, G. Steinbrück, F.M. Stober, M. Stöver, H. Tholen, D. Troendle, E. Usai, L. Vanelderen, A. Vanhoefer, B. Vormwald

JHEP04(2017)018

Institut für Experimentelle Kernphysik, Karlsruhe, Germany

C. Barth, C. Baus, J. Berger, E. Butz, T. Chwalek, F. Colombo, W. De Boer, A. Dierlamm, S. Fink, R. Friese, M. Giffels, A. Gilbert, P. Goldenzweig, D. Haitz, F. Hartmann[16], S.M. Heindl, U. Husemann, I. Katkov[14], P. Lobelle Pardo, B. Maier, H. Mildner, M.U. Mozer, Th. Müller, M. Plagge, G. Quast, K. Rabbertz, S. Röcker, F. Roscher, M. Schröder, I. Shvetsov, G. Sieber, H.J. Simonis, R. Ulrich, J. Wagner-Kuhr, S. Wayand, M. Weber, T. Weiler, S. Williamson, C. Wöhrmann, R. Wolf

Institute of Nuclear and Particle Physics (INPP), NCSR Demokritos, Aghia Paraskevi, Greece

G. Anagnostou, G. Daskalakis, T. Geralis, V.A. Giakoumopoulou, A. Kyriakis, D. Loukas, I. Topsis-Giotis

National and Kapodistrian University of Athens, Athens, Greece

S. Kesisoglou, A. Panagiotou, N. Saoulidou, E. Tziaferi

University of Ioánnina, Ioánnina, Greece

I. Evangelou, G. Flouris, C. Foudas, P. Kokkas, N. Loukas, N. Manthos, I. Papadopoulos, E. Paradas

MTA-ELTE Lendület CMS Particle and Nuclear Physics Group, Eötvös Loránd University, Budapest, Hungary

N. Filipovic

Wigner Research Centre for Physics, Budapest, Hungary

G. Bencze, C. Hajdu, P. Hidas, D. Horvath[20], F. Sikler, V. Veszpremi, G. Vesztergombi[21], A.J. Zsigmond

Institute of Nuclear Research ATOMKI, Debrecen, Hungary

N. Beni, S. Czellar, J. Karancsi[22], A. Makovec, J. Molnar, Z. Szillasi

University of Debrecen, Debrecen, Hungary

M. Bartók[21], P. Raics, Z.L. Trocsanyi, B. Ujvari

National Institute of Science Education and Research, Bhubaneswar, India

S. Bahinipati, S. Choudhury[23], P. Mal, K. Mandal, A. Nayak[24], D.K. Sahoo, N. Sahoo, S.K. Swain

Panjab University, Chandigarh, India

S. Bansal, S.B. Beri, V. Bhatnagar, R. Chawla, U.Bhawandeep, A.K. Kalsi, A. Kaur, M. Kaur, R. Kumar, A. Mehta, M. Mittal, J.B. Singh, G. Walia

University of Delhi, Delhi, India

Ashok Kumar, A. Bhardwaj, B.C. Choudhary, R.B. Garg, S. Keshri, S. Malhotra, M. Naimuddin, N. Nishu, K. Ranjan, R. Sharma, V. Sharma

JHEP04(2017)018

Saha Institute of Nuclear Physics, Kolkata, India

R. Bhattacharya, S. Bhattacharya, K. Chatterjee, S. Dey, S. Dutt, S. Dutta, S. Ghosh, N. Majumdar, A. Modak, K. Mondal, S. Mukhopadhyay, S. Nandan, A. Purohit, A. Roy, D. Roy, S. Roy Chowdhury, S. Sarkar, M. Sharan, S. Thakur

Indian Institute of Technology Madras, Madras, India

P.K. Behera

Bhabha Atomic Research Centre, Mumbai, India

R. Chudasama, D. Dutta, V. Jha, V. Kumar, A.K. Mohanty[16], P.K. Netrakanti, L.M. Pant, P. Shukla, A. Topkar

Tata Institute of Fundamental Research-A, Mumbai, India

T. Aziz, S. Dugad, G. Kole, B. Mahakud, S. Mitra, G.B. Mohanty, B. Parida, N. Sur, B. Sutar

Tata Institute of Fundamental Research-B, Mumbai, India

S. Banerjee, S. Bhowmik[25], R.K. Dewanjee, S. Ganguly, M. Guchait, Sa. Jain, S. Kumar, M. Maity[25], G. Majumder, K. Mazumdar, T. Sarkar[25], N. Wickramage[26]

Indian Institute of Science Education and Research (IISER), Pune, India

S. Chauhan, S. Dube, V. Hegde, A. Kapoor, K. Kothekar, A. Rane, S. Sharma

Institute for Research in Fundamental Sciences (IPM), Tehran, Iran

H. Behnamian, S. Chenarani[27], E. Eskandari Tadavani, S.M. Etesami[27], A. Fahim[28], M. Khakzad, M. Mohammadi Najafabadi, M. Naseri, S. Paktinat Mehdiabadi[29], F. Rezaei Hosseinabadi, B. Safarzadeh[30], M. Zeinali

University College Dublin, Dublin, Ireland

M. Felcini, M. Grunewald

INFN Sezione di Bari [a], Università di Bari [b], Politecnico di Bari [c], Bari, Italy

M. Abbrescia[a,b], C. Calabria[a,b], C. Caputo[a,b], A. Colaleo[a], D. Creanza[a,c], L. Cristella[a,b], N. De Filippis[a,c], M. De Palma[a,b], L. Fiore[a], G. Iaselli[a,c], G. Maggi[a,c], M. Maggi[a], G. Miniello[a,b], S. My[a,b], S. Nuzzo[a,b], A. Pompili[a,b], G. Pugliese[a,c], R. Radogna[a,b], A. Ranieri[a], G. Selvaggi[a,b], L. Silvestris[a,16], R. Venditti[a,b], P. Verwilligen[a]

INFN Sezione di Bologna [a], Università di Bologna [b], Bologna, Italy

G. Abbiendi[a], C. Battilana, D. Bonacorsi[a,b], S. Braibant-Giacomelli[a,b], L. Brigliadori[a,b], R. Campanini[a,b], P. Capiluppi[a,b], A. Castro[a,b], F.R. Cavallo[a], S.S. Chhibra[a,b], G. Codispoti[a,b], M. Cuffiani[a,b], G.M. Dallavalle[a], F. Fabbri[a], A. Fanfani[a,b], D. Fasanella[a,b], P. Giacomelli[a], C. Grandi[a], L. Guiducci[a,b], S. Marcellini[a], G. Masetti[a], A. Montanari[a], F.L. Navarria[a,b], A. Perrotta[a], A.M. Rossi[a,b], T. Rovelli[a,b], G.P. Siroli[a,b], N. Tosi[a,b,16]

INFN Sezione di Catania [a], Università di Catania [b], Catania, Italy

S. Albergo[a,b], M. Chiorboli[a,b], S. Costa[a,b], A. Di Mattia[a], F. Giordano[a,b], R. Potenza[a,b], A. Tricomi[a,b], C. Tuve[a,b]

JHEP04(2017)018

INFN Sezione di Firenze [a], Università di Firenze [b], Firenze, Italy

G. Barbagli[a], V. Ciulli[a,b], C. Civinini[a], R. D'Alessandro[a,b], E. Focardi[a,b], V. Gori[a,b], P. Lenzi[a,b], M. Meschini[a], S. Paoletti[a], G. Sguazzoni[a], L. Viliani[a,b,16]

INFN Laboratori Nazionali di Frascati, Frascati, Italy

L. Benussi, S. Bianco, F. Fabbri, D. Piccolo, F. Primavera[16]

INFN Sezione di Genova [a], Università di Genova [b], Genova, Italy

V. Calvelli[a,b], F. Ferro[a], M. Lo Vetere[a,b], M.R. Monge[a,b], E. Robutti[a], S. Tosi[a,b]

INFN Sezione di Milano-Bicocca [a], Università di Milano-Bicocca [b], Milano, Italy

L. Brianza[16], M.E. Dinardo[a,b], S. Fiorendi[a,b], S. Gennai[a], A. Ghezzi[a,b], P. Govoni[a,b], M. Malberti, S. Malvezzi[a], R.A. Manzoni[a,b,16], B. Marzocchi[a,b], D. Menasce[a], L. Moroni[a], M. Paganoni[a,b], D. Pedrini[a], S. Pigazzini, S. Ragazzi[a,b], T. Tabarelli de Fatis[a,b]

INFN Sezione di Napoli [a], Università di Napoli 'Federico II' [b], Napoli, Italy, Università della Basilicata [c], Potenza, Italy, Università G. Marconi [d], Roma, Italy

S. Buontempo[a], N. Cavallo[a,c], G. De Nardo, S. Di Guida[a,d,16], M. Esposito[a,b], F. Fabozzi[a,c], A.O.M. Iorio[a,b], G. Lanza[a], L. Lista[a], S. Meola[a,d,16], P. Paolucci[a,16], C. Sciacca[a,b], F. Thyssen

INFN Sezione di Padova [a], Università di Padova [b], Padova, Italy, Università di Trento [c], Trento, Italy

P. Azzi[a,16], N. Bacchetta[a], L. Benato[a,b], D. Bisello[a,b], A. Boletti[a,b], R. Carlin[a,b], A. Carvalho Antunes De Oliveira[a,b], P. Checchia[a], M. Dall'Osso[a,b], P. De Castro Manzano[a], T. Dorigo[a], U. Dosselli[a], F. Gasparini[a,b], U. Gasparini[a,b], A. Gozzelino[a], S. Lacaprara[a], M. Margoni[a,b], A.T. Meneguzzo[a,b], J. Pazzini[a,b,16], N. Pozzobon[a,b], P. Ronchese[a,b], F. Simonetto[a,b], E. Torassa[a], M. Zanetti, P. Zotto[a,b], A. Zucchetta[a,b], G. Zumerle[a,b]

INFN Sezione di Pavia [a], Università di Pavia [b], Pavia, Italy

A. Braghieri[a], A. Magnani[a,b], P. Montagna[a,b], S.P. Ratti[a,b], V. Re[a], C. Riccardi[a,b], P. Salvini[a], I. Vai[a,b], P. Vitulo[a,b]

INFN Sezione di Perugia [a], Università di Perugia [b], Perugia, Italy

L. Alunni Solestizi[a,b], G.M. Bilei[a], D. Ciangottini[a,b], L. Fanò[a,b], P. Lariccia[a,b], R. Leonardi[a,b], G. Mantovani[a,b], M. Menichelli[a], A. Saha[a], A. Santocchia[a,b]

INFN Sezione di Pisa [a], Università di Pisa [b], Scuola Normale Superiore di Pisa [c], Pisa, Italy

K. Androsov[a,31], P. Azzurri[a,16], G. Bagliesi[a], J. Bernardini[a], T. Boccali[a], R. Castaldi[a], M.A. Ciocci[a,31], R. Dell'Orso[a], S. Donato[a,c], G. Fedi, A. Giassi[a], M.T. Grippo[a,31], F. Ligabue[a,c], T. Lomtadze[a], L. Martini[a,b], A. Messineo[a,b], F. Palla[a], A. Rizzi[a,b], A. Savoy-Navarro[a,32], P. Spagnolo[a], R. Tenchini[a], G. Tonelli[a,b], A. Venturi[a], P.G. Verdini[a]

JHEP04(2017)018

INFN Sezione di Roma [a], Università di Roma [b], Roma, Italy

L. Barone[a,b], F. Cavallari[a], M. Cipriani[a,b], G. D'imperio[a,b,16], D. Del Re[a,b,16], M. Diemoz[a], S. Gelli[a,b], E. Longo[a,b], F. Margaroli[a,b], P. Meridiani[a], G. Organtini[a,b], R. Paramatti[a], F. Preiato[a,b], S. Rahatlou[a,b], C. Rovelli[a], F. Santanastasio[a,b]

INFN Sezione di Torino [a], Università di Torino [b], Torino, Italy, Università del Piemonte Orientale [c], Novara, Italy

N. Amapane[a,b], R. Arcidiacono[a,c,16], S. Argiro[a,b], M. Arneodo[a,c], N. Bartosik[a], R. Bellan[a,b], C. Biino[a], N. Cartiglia[a], F. Cenna[a,b], M. Costa[a,b], R. Covarelli[a,b], A. Degano[a,b], N. Demaria[a], L. Finco[a,b], B. Kiani[a,b], C. Mariotti[a], S. Maselli[a], E. Migliore[a,b], V. Monaco[a,b], E. Monteil[a,b], M.M. Obertino[a,b], L. Pacher[a,b], N. Pastrone[a], M. Pelliccioni[a], G.L. Pinna Angioni[a,b], F. Ravera[a,b], A. Romero[a,b], M. Ruspa[a,c], R. Sacchi[a,b], K. Shchelina[a,b], V. Sola[a], A. Solano[a,b], A. Staiano[a], P. Traczyk[a,b]

INFN Sezione di Trieste [a], Università di Trieste [b], Trieste, Italy

S. Belforte[a], M. Casarsa[a], F. Cossutti[a], G. Della Ricca[a,b], C. La Licata[a,b], A. Schizzi[a,b], A. Zanetti[a]

Kyungpook National University, Daegu, Korea

D.H. Kim, G.N. Kim, M.S. Kim, S. Lee, S.W. Lee, Y.D. Oh, S. Sekmen, D.C. Son, Y.C. Yang

Chonbuk National University, Jeonju, Korea

A. Lee

Chonnam National University, Institute for Universe and Elementary Particles, Kwangju, Korea

H. Kim

Hanyang University, Seoul, Korea

J.A. Brochero Cifuentes, T.J. Kim

Korea University, Seoul, Korea

S. Cho, S. Choi, Y. Go, D. Gyun, S. Ha, B. Hong, Y. Jo, Y. Kim, B. Lee, K. Lee, K.S. Lee, S. Lee, J. Lim, S.K. Park, Y. Roh

Seoul National University, Seoul, Korea

J. Almond, J. Kim, H. Lee, S.B. Oh, B.C. Radburn-Smith, S.h. Seo, U.K. Yang, H.D. Yoo, G.B. Yu

University of Seoul, Seoul, Korea

M. Choi, H. Kim, J.H. Kim, J.S.H. Lee, I.C. Park, G. Ryu, M.S. Ryu

Sungkyunkwan University, Suwon, Korea

Y. Choi, J. Goh, C. Hwang, J. Lee, I. Yu

Vilnius University, Vilnius, Lithuania

V. Dudenas, A. Juodagalvis, J. Vaitkus

JHEP04(2017)018

National Centre for Particle Physics, Universiti Malaya, Kuala Lumpur, Malaysia

I. Ahmed, Z.A. Ibrahim, J.R. Komaragiri, M.A.B. Md Ali[33], F. Mohamad Idris[34], W.A.T. Wan Abdullah, M.N. Yusli, Z. Zolkapli

Centro de Investigacion y de Estudios Avanzados del IPN, Mexico City, Mexico

H. Castilla-Valdez, E. De La Cruz-Burelo, I. Heredia-De La Cruz[35], A. Hernandez-Almada, R. Lopez-Fernandez, R. Magaña Villalba, J. Mejia Guisao, A. Sanchez-Hernandez

Universidad Iberoamericana, Mexico City, Mexico

S. Carrillo Moreno, C. Oropeza Barrera, F. Vazquez Valencia

Benemerita Universidad Autonoma de Puebla, Puebla, Mexico

S. Carpinteyro, I. Pedraza, H.A. Salazar Ibarguen, C. Uribe Estrada

Universidad Autónoma de San Luis Potosí, San Luis Potosí, Mexico

A. Morelos Pineda

University of Auckland, Auckland, New Zealand

D. Krofcheck

University of Canterbury, Christchurch, New Zealand

P.H. Butler

National Centre for Physics, Quaid-I-Azam University, Islamabad, Pakistan

A. Ahmad, M. Ahmad, Q. Hassan, H.R. Hoorani, W.A. Khan, M.A. Shah, M. Shoaib, M. Waqas

National Centre for Nuclear Research, Swierk, Poland

H. Bialkowska, M. Bluj, B. Boimska, T. Frueboes, M. Górski, M. Kazana, K. Nawrocki, K. Romanowska-Rybinska, M. Szleper, P. Zalewski

Institute of Experimental Physics, Faculty of Physics, University of Warsaw, Warsaw, Poland

K. Bunkowski, A. Byszuk[36], K. Doroba, A. Kalinowski, M. Konecki, J. Krolikowski, M. Misiura, M. Olszewski, M. Walczak

Laboratório de Instrumentação e Física Experimental de Partículas, Lisboa, Portugal

P. Bargassa, C. Beirão Da Cruz E Silva, A. Di Francesco, P. Faccioli, P.G. Ferreira Parracho, M. Gallinaro, J. Hollar, N. Leonardo, L. Lloret Iglesias, M.V. Nemallapudi, J. Rodrigues Antunes, J. Seixas, O. Toldaiev, D. Vadruccio, J. Varela, P. Vischia

Joint Institute for Nuclear Research, Dubna, Russia

I. Belotelov, P. Bunin, M. Gavrilenko, I. Golutvin, I. Gorbunov, V. Karjavin, A. Lanev, A. Malakhov, V. Matveev[37,38], P. Moisenz, V. Palichik, V. Perelygin, M. Savina, S. Shmatov, S. Shulha, N. Skatchkov, V. Smirnov, N. Voytishin, A. Zarubin

JHEP04(2017)018

Petersburg Nuclear Physics Institute, Gatchina (St. Petersburg), Russia
L. Chtchipounov, V. Golovtsov, Y. Ivanov, V. Kim[39], E. Kuznetsova[40], V. Murzin, V. Oreshkin, V. Sulimov, A. Vorobyev

Institute for Nuclear Research, Moscow, Russia
Yu. Andreev, A. Dermenev, S. Gninenko, N. Golubev, A. Karneyeu, M. Kirsanov, N. Krasnikov, A. Pashenkov, D. Tlisov, A. Toropin

Institute for Theoretical and Experimental Physics, Moscow, Russia
V. Epshteyn, V. Gavrilov, N. Lychkovskaya, V. Popov, I. Pozdnyakov, G. Safronov, A. Spiridonov, M. Toms, E. Vlasov, A. Zhokin

Moscow Institute of Physics and Technology
A. Bylinkin[38]

National Research Nuclear University 'Moscow Engineering Physics Institute' (MEPhI), Moscow, Russia
R. Chistov[41], M. Danilov[41], V. Rusinov

P.N. Lebedev Physical Institute, Moscow, Russia
V. Andreev, M. Azarkin[38], I. Dremin[38], M. Kirakosyan, A. Leonidov[38], S.V. Rusakov, A. Terkulov

Skobeltsyn Institute of Nuclear Physics, Lomonosov Moscow State University, Moscow, Russia
A. Baskakov, A. Belyaev, E. Boos, M. Dubinin[42], L. Dudko, A. Ershov, A. Gribushin, V. Klyukhin, O. Kodolova, I. Lokhtin, I. Miagkov, S. Obraztsov, S. Petrushanko, V. Savrin, A. Snigirev

Novosibirsk State University (NSU), Novosibirsk, Russia
V. Blinov[43], Y.Skovpen[43]

State Research Center of Russian Federation, Institute for High Energy Physics, Protvino, Russia
I. Azhgirey, I. Bayshev, S. Bitioukov, D. Elumakhov, V. Kachanov, A. Kalinin, D. Konstantinov, V. Krychkine, V. Petrov, R. Ryutin, A. Sobol, S. Troshin, N. Tyurin, A. Uzunian, A. Volkov

University of Belgrade, Faculty of Physics and Vinca Institute of Nuclear Sciences, Belgrade, Serbia
P. Adzic[44], P. Cirkovic, D. Devetak, M. Dordevic, J. Milosevic, V. Rekovic

Centro de Investigaciones Energéticas Medioambientales y Tecnológicas (CIEMAT), Madrid, Spain
J. Alcaraz Maestre, M. Barrio Luna, E. Calvo, M. Cerrada, M. Chamizo Llatas, N. Colino, B. De La Cruz, A. Delgado Peris, A. Escalante Del Valle, C. Fernandez Bedoya, J.P. Fernández Ramos, J. Flix, M.C. Fouz, P. Garcia-Abia, O. Gonzalez Lopez, S. Goy Lopez, J.M. Hernandez, M.I. Josa, E. Navarro De Martino, A. Pérez-Calero Yzquierdo, J. Puerta Pelayo, A. Quintario Olmeda, I. Redondo, L. Romero, M.S. Soares

JHEP04(2017)018

Universidad Autónoma de Madrid, Madrid, Spain

J.F. de Trocóniz, M. Missiroli, D. Moran

Universidad de Oviedo, Oviedo, Spain

J. Cuevas, J. Fernandez Menendez, I. Gonzalez Caballero, J.R. González Fernández, E. Palencia Cortezon, S. Sanchez Cruz, I. Suárez Andrés, J.M. Vizan Garcia

Instituto de Física de Cantabria (IFCA), CSIC-Universidad de Cantabria, Santander, Spain

I.J. Cabrillo, A. Calderon, J.R. Castiñeiras De Saa, E. Curras, M. Fernandez, J. Garcia-Ferrero, G. Gomez, A. Lopez Virto, J. Marco, C. Martinez Rivero, F. Matorras, J. Piedra Gomez, T. Rodrigo, A. Ruiz-Jimeno, L. Scodellaro, N. Trevisani, I. Vila, R. Vilar Cortabitarte

CERN, European Organization for Nuclear Research, Geneva, Switzerland

D. Abbaneo, E. Auffray, G. Auzinger, M. Bachtis, P. Baillon, A.H. Ball, D. Barney, P. Bloch, A. Bocci, A. Bonato, C. Botta, T. Camporesi, R. Castello, M. Cepeda, G. Cerminara, M. D'Alfonso, D. d'Enterria, A. Dabrowski, V. Daponte, A. David, M. De Gruttola, A. De Roeck, E. Di Marco[45], M. Dobson, B. Dorney, T. du Pree, D. Duggan, M. Dünser, N. Dupont, A. Elliott-Peisert, S. Fartoukh, G. Franzoni, J. Fulcher, W. Funk, D. Gigi, K. Gill, M. Girone, F. Glege, D. Gulhan, S. Gundacker, M. Guthoff, J. Hammer, P. Harris, J. Hegeman, V. Innocente, P. Janot, J. Kieseler, H. Kirschenmann, V. Knünz, A. Kornmayer[16], M.J. Kortelainen, K. Kousouris, M. Krammer[1], C. Lange, P. Lecoq, C. Lourenço, M.T. Lucchini, L. Malgeri, M. Mannelli, A. Martelli, F. Meijers, J.A. Merlin, S. Mersi, E. Meschi, F. Moortgat, S. Morovic, M. Mulders, H. Neugebauer, S. Orfanelli, L. Orsini, L. Pape, E. Perez, M. Peruzzi, A. Petrilli, G. Petrucciani, A. Pfeiffer, M. Pierini, A. Racz, T. Reis, G. Rolandi[46], M. Rovere, M. Ruan, H. Sakulin, J.B. Sauvan, C. Schäfer, C. Schwick, M. Seidel, A. Sharma, P. Silva, P. Sphicas[47], J. Steggemann, M. Stoye, Y. Takahashi, M. Tosi, D. Treille, A. Triossi, A. Tsirou, V. Veckalns[48], G.I. Veres[21], N. Wardle, A. Zagozdzinska[36], W.D. Zeuner

Paul Scherrer Institut, Villigen, Switzerland

W. Bertl, K. Deiters, W. Erdmann, R. Horisberger, Q. Ingram, H.C. Kaestli, D. Kotlinski, U. Langenegger, T. Rohe

Institute for Particle Physics, ETH Zurich, Zurich, Switzerland

F. Bachmair, L. Bäni, L. Bianchini, B. Casal, G. Dissertori, M. Dittmar, M. Donegà, P. Eller, C. Grab, C. Heidegger, D. Hits, J. Hoss, G. Kasieczka, P. Lecomte†, W. Lustermann, B. Mangano, M. Marionneau, P. Martinez Ruiz del Arbol, M. Masciovecchio, M.T. Meinhard, D. Meister, F. Micheli, P. Musella, F. Nessi-Tedaldi, F. Pandolfi, J. Pata, F. Pauss, G. Perrin, L. Perrozzi, M. Quittnat, M. Rossini, M. Schönenberger, A. Starodumov[49], V.R. Tavolaro, K. Theofilatos, R. Wallny

Universität Zürich, Zurich, Switzerland

T.K. Aarrestad, C. Amsler[50], L. Caminada, M.F. Canelli, A. De Cosa, C. Galloni, A. Hinzmann, T. Hreus, B. Kilminster, J. Ngadiuba, D. Pinna, G. Rauco, P. Robmann,

JHEP04(2017)018

D. Salerno, Y. Yang

National Central University, Chung-Li, Taiwan

V. Candelise, T.H. Doan, Sh. Jain, R. Khurana, M. Konyushikhin, C.M. Kuo, W. Lin, Y.J. Lu, A. Pozdnyakov, S.S. Yu

National Taiwan University (NTU), Taipei, Taiwan

Arun Kumar, P. Chang, Y.H. Chang, Y.W. Chang, Y. Chao, K.F. Chen, P.H. Chen, C. Dietz, F. Fiori, W.-S. Hou, Y. Hsiung, Y.F. Liu, R.-S. Lu, M. Miñano Moya, E. Paganis, A. Psallidas, J.f. Tsai, Y.M. Tzeng

Chulalongkorn University, Faculty of Science, Department of Physics, Bangkok, Thailand

B. Asavapibhop, G. Singh, N. Srimanobhas, N. Suwonjandee

Cukurova University, Adana, Turkey

M.N. Bakirci[51], S. Cerci[52], S. Damarseckin, Z.S. Demiroglu, C. Dozen, I. Dumanoglu, S. Girgis, G. Gokbulut, Y. Guler, E. Gurpinar, I. Hos, E.E. Kangal[53], O. Kara, A. Kayis Topaksu, U. Kiminsu, M. Oglakci, G. Onengut[54], K. Ozdemir[55], B. Tali[52], S. Turkcapar, I.S. Zorbakir, C. Zorbilmez

Middle East Technical University, Physics Department, Ankara, Turkey

B. Bilin, S. Bilmis, B. Isildak[56], G. Karapinar[57], M. Yalvac, M. Zeyrek

Bogazici University, Istanbul, Turkey

E. Gülmez, M. Kaya[58], O. Kaya[59], E.A. Yetkin[60], T. Yetkin[61]

Istanbul Technical University, Istanbul, Turkey

A. Cakir, K. Cankocak, S. Sen[62]

Institute for Scintillation Materials of National Academy of Science of Ukraine, Kharkov, Ukraine

B. Grynyov

National Scientific Center, Kharkov Institute of Physics and Technology, Kharkov, Ukraine

L. Levchuk, P. Sorokin

University of Bristol, Bristol, United Kingdom

R. Aggleton, F. Ball, L. Beck, J.J. Brooke, D. Burns, E. Clement, D. Cussans, H. Flacher, J. Goldstein, M. Grimes, G.P. Heath, H.F. Heath, J. Jacob, L. Kreczko, C. Lucas, D.M. Newbold[63], S. Paramesvaran, A. Poll, T. Sakuma, S. Seif El Nasr-storey, D. Smith, V.J. Smith

Rutherford Appleton Laboratory, Didcot, United Kingdom

D. Barducci, K.W. Bell, A. Belyaev[64], C. Brew, R.M. Brown, L. Calligaris, D. Cieri, D.J.A. Cockerill, J.A. Coughlan, K. Harder, S. Harper, E. Olaiya, D. Petyt, C.H. Shepherd-Themistocleous, A. Thea, I.R. Tomalin, T. Williams

JHEP04(2017)018

Imperial College, London, United Kingdom

M. Baber, R. Bainbridge, O. Buchmuller, A. Bundock, D. Burton, S. Casasso, M. Citron, D. Colling, L. Corpe, P. Dauncey, G. Davies, A. De Wit, M. Della Negra, R. Di Maria, P. Dunne, A. Elwood, D. Futyan, Y. Haddad, G. Hall, G. Iles, T. James, R. Lane, C. Laner, R. Lucas[63], L. Lyons, A.-M. Magnan, S. Malik, L. Mastrolorenzo, J. Nash, A. Nikitenko[49], J. Pela, B. Penning, M. Pesaresi, D.M. Raymond, A. Richards, A. Rose, C. Seez, S. Summers, A. Tapper, K. Uchida, M. Vazquez Acosta[65], T. Virdee[16], J. Wright, S.C. Zenz

Brunel University, Uxbridge, United Kingdom

J.E. Cole, P.R. Hobson, A. Khan, P. Kyberd, D. Leslie, I.D. Reid, P. Symonds, L. Teodorescu, M. Turner

Baylor University, Waco, U.S.A.

A. Borzou, K. Call, J. Dittmann, K. Hatakeyama, H. Liu, N. Pastika

The University of Alabama, Tuscaloosa, U.S.A.

O. Charaf, S.I. Cooper, C. Henderson, P. Rumerio, C. West

Boston University, Boston, U.S.A.

D. Arcaro, A. Avetisyan, T. Bose, D. Gastler, D. Rankin, C. Richardson, J. Rohlf, L. Sulak, D. Zou

Brown University, Providence, U.S.A.

G. Benelli, E. Berry, D. Cutts, A. Garabedian, J. Hakala, U. Heintz, J.M. Hogan, O. Jesus, E. Laird, G. Landsberg, Z. Mao, M. Narain, S. Piperov, S. Sagir, E. Spencer, R. Syarif

University of California, Davis, Davis, U.S.A.

R. Breedon, G. Breto, D. Burns, M. Calderon De La Barca Sanchez, S. Chauhan, M. Chertok, J. Conway, R. Conway, P.T. Cox, R. Erbacher, C. Flores, G. Funk, M. Gardner, W. Ko, R. Lander, C. Mclean, M. Mulhearn, D. Pellett, J. Pilot, F. Ricci-Tam, S. Shalhout, J. Smith, M. Squires, D. Stolp, M. Tripathi, S. Wilbur, R. Yohay

University of California, Los Angeles, U.S.A.

R. Cousins, P. Everaerts, A. Florent, J. Hauser, M. Ignatenko, D. Saltzberg, E. Takasugi, V. Valuev, M. Weber

University of California, Riverside, Riverside, U.S.A.

K. Burt, R. Clare, J. Ellison, J.W. Gary, G. Hanson, J. Heilman, P. Jandir, E. Kennedy, F. Lacroix, O.R. Long, M. Olmedo Negrete, M.I. Paneva, A. Shrinivas, W. Si, H. Wei, S. Wimpenny, B. R. Yates

University of California, San Diego, La Jolla, U.S.A.

J.G. Branson, G.B. Cerati, S. Cittolin, M. Derdzinski, R. Gerosa, A. Holzner, D. Klein, V. Krutelyov, J. Letts, I. Macneill, D. Olivito, S. Padhi, M. Pieri, M. Sani, V. Sharma, S. Simon, M. Tadel, A. Vartak, S. Wasserbaech[66], C. Welke, J. Wood, F. Würthwein, A. Yagil, G. Zevi Della Porta

JHEP04(2017)018

University of California, Santa Barbara - Department of Physics, Santa Barbara, U.S.A.

R. Bhandari, J. Bradmiller-Feld, C. Campagnari, A. Dishaw, V. Dutta, K. Flowers, M. Franco Sevilla, P. Geffert, C. George, F. Golf, L. Gouskos, J. Gran, R. Heller, J. Incandela, N. Mccoll, S.D. Mullin, A. Ovcharova, J. Richman, D. Stuart, I. Suarez, J. Yoo

California Institute of Technology, Pasadena, U.S.A.

D. Anderson, A. Apresyan, J. Bendavid, A. Bornheim, J. Bunn, Y. Chen, J. Duarte, J.M. Lawhorn, A. Mott, H.B. Newman, C. Pena, M. Spiropulu, J.R. Vlimant, S. Xie, R.Y. Zhu

Carnegie Mellon University, Pittsburgh, U.S.A.

M.B. Andrews, V. Azzolini, T. Ferguson, M. Paulini, J. Russ, M. Sun, H. Vogel, I. Vorobiev

University of Colorado Boulder, Boulder, U.S.A.

J.P. Cumalat, W.T. Ford, F. Jensen, A. Johnson, M. Krohn, T. Mulholland, K. Stenson, S.R. Wagner

Cornell University, Ithaca, U.S.A.

J. Alexander, J. Chaves, J. Chu, S. Dittmer, K. Mcdermott, N. Mirman, G. Nicolas Kaufman, J.R. Patterson, A. Rinkevicius, A. Ryd, L. Skinnari, L. Soffi, S.M. Tan, Z. Tao, J. Thom, J. Tucker, P. Wittich, M. Zientek

Fairfield University, Fairfield, U.S.A.

D. Winn

Fermi National Accelerator Laboratory, Batavia, U.S.A.

S. Abdullin, M. Albrow, G. Apollinari, S. Banerjee, L.A.T. Bauerdick, A. Beretvas, J. Berryhill, P.C. Bhat, G. Bolla, K. Burkett, J.N. Butler, H.W.K. Cheung, F. Chlebana, S. Cihangir†, M. Cremonesi, V.D. Elvira, I. Fisk, J. Freeman, E. Gottschalk, L. Gray, D. Green, S. Grünendahl, O. Gutsche, D. Hare, R.M. Harris, S. Hasegawa, J. Hirschauer, Z. Hu, B. Jayatilaka, S. Jindariani, M. Johnson, U. Joshi, B. Klima, B. Kreis, S. Lammel, J. Linacre, D. Lincoln, R. Lipton, T. Liu, R. Lopes De Sá, J. Lykken, K. Maeshima, N. Magini, J.M. Marraffino, S. Maruyama, D. Mason, P. McBride, P. Merkel, S. Mrenna, S. Nahn, C. Newman-Holmes†, V. O'Dell, K. Pedro, O. Prokofyev, G. Rakness, L. Ristori, E. Sexton-Kennedy, A. Soha, W.J. Spalding, L. Spiegel, S. Stoynev, N. Strobbe, L. Taylor, S. Tkaczyk, N.V. Tran, L. Uplegger, E.W. Vaandering, C. Vernieri, M. Verzocchi, R. Vidal, M. Wang, H.A. Weber, A. Whitbeck

University of Florida, Gainesville, U.S.A.

D. Acosta, P. Avery, P. Bortignon, D. Bourilkov, A. Brinkerhoff, A. Carnes, M. Carver, D. Curry, S. Das, R.D. Field, I.K. Furic, J. Konigsberg, A. Korytov, P. Ma, K. Matchev, H. Mei, P. Milenovic[67], G. Mitselmakher, D. Rank, L. Shchutska, D. Sperka, L. Thomas, J. Wang, S. Wang, J. Yelton

Florida International University, Miami, U.S.A.

S. Linn, P. Markowitz, G. Martinez, J.L. Rodriguez

JHEP04(2017)018

Florida State University, Tallahassee, U.S.A.

A. Ackert, J.R. Adams, T. Adams, A. Askew, S. Bein, B. Diamond, S. Hagopian, V. Hagopian, K.F. Johnson, A. Khatiwada, H. Prosper, A. Santra, M. Weinberg

Florida Institute of Technology, Melbourne, U.S.A.

M.M. Baarmand, V. Bhopatkar, S. Colafranceschi[68], M. Hohlmann, D. Noonan, T. Roy, F. Yumiceva

University of Illinois at Chicago (UIC), Chicago, U.S.A.

M.R. Adams, L. Apanasevich, D. Berry, R.R. Betts, I. Bucinskaite, R. Cavanaugh, O. Evdokimov, L. Gauthier, C.E. Gerber, D.J. Hofman, P. Kurt, C. O'Brien, I.D. Sandoval Gonzalez, P. Turner, N. Varelas, H. Wang, Z. Wu, M. Zakaria, J. Zhang

The University of Iowa, Iowa City, U.S.A.

B. Bilki[69], W. Clarida, K. Dilsiz, S. Durgut, R.P. Gandrajula, M. Haytmyradov, V. Khristenko, J.-P. Merlo, H. Mermerkaya[70], A. Mestvirishvili, A. Moeller, J. Nachtman, H. Ogul, Y. Onel, F. Ozok[71], A. Penzo, C. Snyder, E. Tiras, J. Wetzel, K. Yi

Johns Hopkins University, Baltimore, U.S.A.

I. Anderson, B. Blumenfeld, A. Cocoros, N. Eminizer, D. Fehling, L. Feng, A.V. Gritsan, P. Maksimovic, M. Osherson, J. Roskes, U. Sarica, M. Swartz, M. Xiao, Y. Xin, C. You

The University of Kansas, Lawrence, U.S.A.

A. Al-bataineh, P. Baringer, A. Bean, S. Boren, J. Bowen, C. Bruner, J. Castle, L. Forthomme, R.P. Kenny III, A. Kropivnitskaya, D. Majumder, W. Mcbrayer, M. Murray, S. Sanders, R. Stringer, J.D. Tapia Takaki, Q. Wang

Kansas State University, Manhattan, U.S.A.

A. Ivanov, K. Kaadze, S. Khalil, M. Makouski, Y. Maravin, A. Mohammadi, L.K. Saini, N. Skhirtladze, S. Toda

Lawrence Livermore National Laboratory, Livermore, U.S.A.

F. Rebassoo, D. Wright

University of Maryland, College Park, U.S.A.

C. Anelli, A. Baden, O. Baron, A. Belloni, B. Calvert, S.C. Eno, C. Ferraioli, J.A. Gomez, N.J. Hadley, S. Jabeen, R.G. Kellogg, T. Kolberg, J. Kunkle, Y. Lu, A.C. Mignerey, Y.H. Shin, A. Skuja, M.B. Tonjes, S.C. Tonwar

Massachusetts Institute of Technology, Cambridge, U.S.A.

D. Abercrombie, B. Allen, A. Apyan, R. Barbieri, A. Baty, R. Bi, K. Bierwagen, S. Brandt, W. Busza, I.A. Cali, Z. Demiragli, L. Di Matteo, G. Gomez Ceballos, M. Goncharov, D. Hsu, Y. Iiyama, G.M. Innocenti, M. Klute, D. Kovalskyi, K. Krajczar, Y.S. Lai, Y.-J. Lee, A. Levin, P.D. Luckey, A.C. Marini, C. Mcginn, C. Mironov, S. Narayanan, X. Niu, C. Paus, C. Roland, G. Roland, J. Salfeld-Nebgen, G.S.F. Stephans, K. Sumorok, K. Tatar, M. Varma, D. Velicanu, J. Veverka, J. Wang, T.W. Wang, B. Wyslouch, M. Yang, V. Zhukova

JHEP04(2017)018

University of Minnesota, Minneapolis, U.S.A.

A.C. Benvenuti, R.M. Chatterjee, A. Evans, A. Finkel, A. Gude, P. Hansen, S. Kalafut, S.C. Kao, Y. Kubota, Z. Lesko, J. Mans, S. Nourbakhsh, N. Ruckstuhl, R. Rusack, N. Tambe, J. Turkewitz

University of Mississippi, Oxford, U.S.A.

J.G. Acosta, S. Oliveros

University of Nebraska-Lincoln, Lincoln, U.S.A.

E. Avdeeva, R. Bartek, K. Bloom, D.R. Claes, A. Dominguez, C. Fangmeier, R. Gonzalez Suarez, R. Kamalieddin, I. Kravchenko, A. Malta Rodrigues, F. Meier, J. Monroy, J.E. Siado, G.R. Snow, B. Stieger

State University of New York at Buffalo, Buffalo, U.S.A.

M. Alyari, J. Dolen, J. George, A. Godshalk, C. Harrington, I. Iashvili, J. Kaisen, A. Kharchilava, A. Kumar, A. Parker, S. Rappoccio, B. Roozbahani

Northeastern University, Boston, U.S.A.

G. Alverson, E. Barberis, D. Baumgartel, A. Hortiangtham, A. Massironi, D.M. Morse, D. Nash, T. Orimoto, R. Teixeira De Lima, D. Trocino, R.-J. Wang, D. Wood

Northwestern University, Evanston, U.S.A.

S. Bhattacharya, K.A. Hahn, A. Kubik, A. Kumar, J.F. Low, N. Mucia, N. Odell, B. Pollack, M.H. Schmitt, K. Sung, M. Trovato, M. Velasco

University of Notre Dame, Notre Dame, U.S.A.

N. Dev, M. Hildreth, K. Hurtado Anampa, C. Jessop, D.J. Karmgard, N. Kellams, K. Lannon, N. Marinelli, F. Meng, C. Mueller, Y. Musienko[37], M. Planer, A. Reinsvold, R. Ruchti, G. Smith, S. Taroni, M. Wayne, M. Wolf, A. Woodard

The Ohio State University, Columbus, U.S.A.

J. Alimena, L. Antonelli, J. Brinson, B. Bylsma, L.S. Durkin, S. Flowers, B. Francis, A. Hart, C. Hill, R. Hughes, W. Ji, B. Liu, W. Luo, D. Puigh, B.L. Winer, H.W. Wulsin

Princeton University, Princeton, U.S.A.

S. Cooperstein, O. Driga, P. Elmer, J. Hardenbrook, P. Hebda, D. Lange, J. Luo, D. Marlow, T. Medvedeva, K. Mei, M. Mooney, J. Olsen, C. Palmer, P. Piroué, D. Stickland, C. Tully, A. Zuranski

University of Puerto Rico, Mayaguez, U.S.A.

S. Malik

Purdue University, West Lafayette, U.S.A.

A. Barker, V.E. Barnes, S. Folgueras, L. Gutay, M.K. Jha, M. Jones, A.W. Jung, K. Jung, D.H. Miller, N. Neumeister, X. Shi, J. Sun, A. Svyatkovskiy, F. Wang, W. Xie, L. Xu

Purdue University Calumet, Hammond, U.S.A.

N. Parashar, J. Stupak

JHEP04(2017)018

Rice University, Houston, U.S.A.

A. Adair, B. Akgun, Z. Chen, K.M. Ecklund, F.J.M. Geurts, M. Guilbaud, W. Li, B. Michlin, M. Northup, B.P. Padley, R. Redjimi, J. Roberts, J. Rorie, Z. Tu, J. Zabel

University of Rochester, Rochester, U.S.A.

B. Betchart, A. Bodek, P. de Barbaro, R. Demina, Y.t. Duh, T. Ferbel, M. Galanti, A. Garcia-Bellido, J. Han, O. Hindrichs, A. Khukhunaishvili, K.H. Lo, P. Tan, M. Verzetti

Rutgers, The State University of New Jersey, Piscataway, U.S.A.

A. Agapitos, J.P. Chou, E. Contreras-Campana, Y. Gershtein, T.A. Gómez Espinosa, E. Halkiadakis, M. Heindl, D. Hidas, E. Hughes, S. Kaplan, R. Kunnawalkam Elayavalli, S. Kyriacou, A. Lath, K. Nash, H. Saka, S. Salur, S. Schnetzer, D. Sheffield, S. Somalwar, R. Stone, S. Thomas, P. Thomassen, M. Walker

University of Tennessee, Knoxville, U.S.A.

M. Foerster, J. Heideman, G. Riley, K. Rose, S. Spanier, K. Thapa

Texas A&M University, College Station, U.S.A.

O. Bouhali[72], A. Celik, M. Dalchenko, M. De Mattia, A. Delgado, S. Dildick, R. Eusebi, J. Gilmore, T. Huang, E. Juska, T. Kamon[73], R. Mueller, Y. Pakhotin, R. Patel, A. Perloff, L. Perniè, D. Rathjens, A. Rose, A. Safonov, A. Tatarinov, K.A. Ulmer

Texas Tech University, Lubbock, U.S.A.

N. Akchurin, C. Cowden, J. Damgov, F. De Guio, C. Dragoiu, P.R. Dudero, J. Faulkner, S. Kunori, K. Lamichhane, S.W. Lee, T. Libeiro, T. Peltola, S. Undleeb, I. Volobouev, Z. Wang

Vanderbilt University, Nashville, U.S.A.

A.G. Delannoy, S. Greene, A. Gurrola, R. Janjam, W. Johns, C. Maguire, A. Melo, H. Ni, P. Sheldon, S. Tuo, J. Velkovska, Q. Xu

University of Virginia, Charlottesville, U.S.A.

M.W. Arenton, P. Barria, B. Cox, J. Goodell, R. Hirosky, A. Ledovskoy, H. Li, C. Neu, T. Sinthuprasith, X. Sun, Y. Wang, E. Wolfe, F. Xia

Wayne State University, Detroit, U.S.A.

C. Clarke, R. Harr, P.E. Karchin, P. Lamichhane, J. Sturdy

University of Wisconsin - Madison, Madison, WI, U.S.A.

D.A. Belknap, S. Dasu, L. Dodd, S. Duric, B. Gomber, M. Grothe, M. Herndon, A. Hervé, P. Klabbers, A. Lanaro, A. Levine, K. Long, R. Loveless, I. Ojalvo, T. Perry, G. Polese, T. Ruggles, A. Savin, N. Smith, W.H. Smith, D. Taylor, N. Woods

†: Deceased

1: Also at Vienna University of Technology, Vienna, Austria

2: Also at State Key Laboratory of Nuclear Physics and Technology, Peking University, Beijing, China

JHEP04(2017)018

3: Also at Institut Pluridisciplinaire Hubert Curien, Université de Strasbourg, Université de Haute Alsace Mulhouse, CNRS/IN2P3, Strasbourg, France
4: Also at Universidade Estadual de Campinas, Campinas, Brazil
5: Also at Universidade Federal de Pelotas, Pelotas, Brazil
6: Also at Université Libre de Bruxelles, Bruxelles, Belgium
7: Also at Deutsches Elektronen-Synchrotron, Hamburg, Germany
8: Also at Joint Institute for Nuclear Research, Dubna, Russia
9: Also at Cairo University, Cairo, Egypt
10: Also at Fayoum University, El-Fayoum, Egypt
11: Now at British University in Egypt, Cairo, Egypt
12: Now at Ain Shams University, Cairo, Egypt
13: Also at Université de Haute Alsace, Mulhouse, France
14: Also at Skobeltsyn Institute of Nuclear Physics, Lomonosov Moscow State University, Moscow, Russia
15: Also at Tbilisi State University, Tbilisi, Georgia
16: Also at CERN, European Organization for Nuclear Research, Geneva, Switzerland
17: Also at RWTH Aachen University, III. Physikalisches Institut A, Aachen, Germany
18: Also at University of Hamburg, Hamburg, Germany
19: Also at Brandenburg University of Technology, Cottbus, Germany
20: Also at Institute of Nuclear Research ATOMKI, Debrecen, Hungary
21: Also at MTA-ELTE Lendület CMS Particle and Nuclear Physics Group, Eötvös Loránd University, Budapest, Hungary
22: Also at University of Debrecen, Debrecen, Hungary
23: Also at Indian Institute of Science Education and Research, Bhopal, India
24: Also at Institute of Physics, Bhubaneswar, India
25: Also at University of Visva-Bharati, Santiniketan, India
26: Also at University of Ruhuna, Matara, Sri Lanka
27: Also at Isfahan University of Technology, Isfahan, Iran
28: Also at University of Tehran, Department of Engineering Science, Tehran, Iran
29: Also at Yazd University, Yazd, Iran
30: Also at Plasma Physics Research Center, Science and Research Branch, Islamic Azad University, Tehran, Iran
31: Also at Università degli Studi di Siena, Siena, Italy
32: Also at Purdue University, West Lafayette, U.S.A.
33: Also at International Islamic University of Malaysia, Kuala Lumpur, Malaysia
34: Also at Malaysian Nuclear Agency, MOSTI, Kajang, Malaysia
35: Also at Consejo Nacional de Ciencia y Tecnología, Mexico city, Mexico
36: Also at Warsaw University of Technology, Institute of Electronic Systems, Warsaw, Poland
37: Also at Institute for Nuclear Research, Moscow, Russia
38: Now at National Research Nuclear University 'Moscow Engineering Physics Institute' (MEPhI), Moscow, Russia
39: Also at St. Petersburg State Polytechnical University, St. Petersburg, Russia
40: Also at University of Florida, Gainesville, U.S.A.
41: Also at P.N. Lebedev Physical Institute, Moscow, Russia
42: Also at California Institute of Technology, Pasadena, U.S.A.
43: Also at Budker Institute of Nuclear Physics, Novosibirsk, Russia
44: Also at Faculty of Physics, University of Belgrade, Belgrade, Serbia
45: Also at INFN Sezione di Roma; Università di Roma, Roma, Italy

JHEP04(2017)018

46: Also at Scuola Normale e Sezione dell'INFN, Pisa, Italy
47: Also at National and Kapodistrian University of Athens, Athens, Greece
48: Also at Riga Technical University, Riga, Latvia
49: Also at Institute for Theoretical and Experimental Physics, Moscow, Russia
50: Also at Albert Einstein Center for Fundamental Physics, Bern, Switzerland
51: Also at Gaziosmanpasa University, Tokat, Turkey
52: Also at Adiyaman University, Adiyaman, Turkey
53: Also at Mersin University, Mersin, Turkey
54: Also at Cag University, Mersin, Turkey
55: Also at Piri Reis University, Istanbul, Turkey
56: Also at Ozyegin University, Istanbul, Turkey
57: Also at Izmir Institute of Technology, Izmir, Turkey
58: Also at Marmara University, Istanbul, Turkey
59: Also at Kafkas University, Kars, Turkey
60: Also at Istanbul Bilgi University, Istanbul, Turkey
61: Also at Yildiz Technical University, Istanbul, Turkey
62: Also at Hacettepe University, Ankara, Turkey
63: Also at Rutherford Appleton Laboratory, Didcot, United Kingdom
64: Also at School of Physics and Astronomy, University of Southampton, Southampton, United Kingdom
65: Also at Instituto de Astrofísica de Canarias, La Laguna, Spain
66: Also at Utah Valley University, Orem, U.S.A.
67: Also at University of Belgrade, Faculty of Physics and Vinca Institute of Nuclear Sciences, Belgrade, Serbia
68: Also at Facoltà Ingegneria, Università di Roma, Roma, Italy
69: Also at Argonne National Laboratory, Argonne, U.S.A.
70: Also at Erzincan University, Erzincan, Turkey
71: Also at Mimar Sinan University, Istanbul, Istanbul, Turkey
72: Also at Texas A&M University at Qatar, Doha, Qatar
73: Also at Kyungpook National University, Daegu, Korea

JHEP04(2017)018